Ceramics Division

FY 2003 Programs and Accomplishments




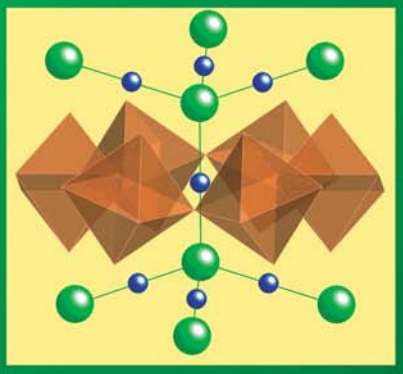

MSEL

NIST
National Institute of Standards and Technology
Technology Administration
U.S. Department of Commerce
NISTIR 7014
September 2003

On the Cover:

From the front cover and continuing on to the back, the images shown are, respectively:

Fig 1 - Pyrochlore and pyrochlore-related compounds occurring in the Bi_2O_3-ZnO-Nb_2O_5 system are attractive candidates for capacitor and high-frequency filter applications in multilayer structures co-fired with metal electrodes. Illustrated is the pyrochlore-type crystal structure $A_2B_2O_7$, where A (blue) represents a large cation and B represents a smaller cation occupying octahedra (orange) formed by oxygen ions. The structural formula is often written as $B_2O_6 \bullet A_2O'$, which emphasizes that the arrangement consists of two interpenetrating networks of vertex-linked octahedra (B_2O_6), and a cuprite-like A_2O' tetrahedral net, represented here by the green (O´) and blue (A) spheres. (See also the highlight "Crystal Chemistry of Novel Wireless Dielectrics: Bi-Zn-Nb-O Pyrochlores.")

Fig 2 - Plumes from the dual-beam, dual-target pulsed laser deposition facility. The yellow plume is from a barium titanate target and the blue plume is from a strontium titanate target. A compositonally-graded library film is grown on a substrate, positioned in front of the targets, by this technique. (See also the project report "Combinatorial Tools for Materials Science.")

Fig 3 - Temperature (front) and heat flux distribution in a simulated zigzag pore microstructure, such as would be produced by an electron-beam directed-vapor-deposition (EB-DVD) process for depositing thermal barrier coatings. The thermal simulations were performed with the NIST Object-Oriented Finite Element (OOF) analysis software by imposing a 100 ºC temperature gradient across the coating and computing the temperature profile and heat flux. The simulated microstructure was produced using a kinetic Monte Carlo method courtesy of Y. G. Yang and H. N. G. Wadley of the University of Virginia. The substrate was periodically inclined to a vapor flux with a modified cosine distribution to produce the zigzag microstructure.

Fig 4 - Dielectric ceramic resonators, or "talking ceramics," are used in cellular base stations to store and transmit signals to handheld devices such as cell phones. The discovery of this class of ceramic materials, which exhibit high dielectric constants and temperature-stable resonance frequencies, permitted the miniaturization of air-based systems to practical sizes needed for commercially viable base stations. (See also the project report "Phase Equilibria and Properties of Dielectric Ceramics.")

National Institute of Standards and Technology
Arden L. Bement, Jr.
Director

Technology Administration
Phillip J. Bond
Undersecretary of Commerce for Technology

U.S. Department of Commerce
Donald L. Evans
Secretary

Materials Science and Engineering Laboratory

FY 2003 Programs and Accomplishments

Ceramics Division

Debra L. Kaiser, Chief

NISTIR 7014

September 2003

Table of Contents

Table of Contents

Executive Summary

Ceramic materials — *inorganic nonmetals* — have diverse functionality and chemical and mechanical robustness that makes them attractive candidates for integration in devices and components for high-end applications including electronics, telecommunications, and biotechnology. Once used predominantly in bulk, monolithic form, ceramic materials are now increasingly used in microscale or even nanoscale forms, such as multilayers, composites, particulates, fibers, and tubes. The NIST Ceramics Division in the Materials Science and Engineering Laboratory (MSEL) is increasingly focusing on the measurements, standards, and data needs for advanced applications of ceramics, particularly in the nanoscale realm.

This report of the Ceramics Division's technical activities in FY 2003 (October 1, 2002–September 30, 2003) contains brief synopses of our projects related to six of the nine umbrella programs in MSEL — Combinatorial Methods, Data and Data Delivery, Materials for Micro- and Opto-Electronics, Materials Property Measurements, Materials Structure Characterization, and Nanocharacterization. Six particularly significant accomplishments are described in more detail in the Technical Highlights section of this report.

The first highlight showcases our division's unique synchrotron radiation facilities at the Advanced Photon Source, specifically, an ultra-small-angle x-ray scattering (USAXS) imaging technique developed by MSEL scientists. Recent results demonstrate that USAXS imaging is a powerful method for obtaining three-dimensional microstructural information on human and artificial tissues that cannot be obtained by conventional x-ray imaging methods.

Critical evaluation of data and data delivery continue to be a cornerstone of the division's activities. The next technical highlight describes the recently published NIST Recommended Practice Guide, *Data Evaluation Theory and Practice for Materials Properties*, the first comprehensive treatise ever written on this subject. In this Guide, formal principles of data evaluation are first established and then applied in an extensive collection of examples drawn primarily from work in the Ceramics Division. Another technical highlight in evaluated data concerns the Inorganic Crystal Structure Database (ICSD), a compendium of three-dimensional crystal structure information for inorganic compounds that was jointly developed with our partners in FIZ-Karlsruhe, Germany. The first release of the Windows-based product for the ICSD earlier this year will greatly increase the accessibility of the information to researchers and instrument manufacturers for materials design, compound identification, and property prediction.

The next two technical highlights focus on research results relevant to the use of ceramic materials for information technology systems. The first of these highlights describes a detailed analysis of the crystal chemistry and the structural origin of the dielectric response in bismuth-based pyrochlores, attractive candidate materials for wireless consumer devices. A new crystal–chemical mechanism for the accommodation of small cations in these compounds was established, and the new principle was applied to pyrochlore structures in other materials systems of interest for communications. The other highlight focuses on metrology for local residual stress determination in III-V multilayer thin film systems for optoelectronics and microelectronics. A novel approach, coupling Raman spectroscopy and photoluminescence measurements, was successfully used to simultaneously determine composition and biaxial stress state in $Al_xGa_{1-x}As$ films.

The final highlight describes a novel master calibration technique for determining the average molecular thickness of a complex hydrocarbon lubricant mixture on magnetic hard disks. The approach may be applied to a variety of engineered surfaces protected by complex hydrocarbon films.

Those who wish to obtain further information about our technical activities may refer to the list of publications following our project synopses, or you may contact the staff or guest researchers listed at the back of this report. Please contact me if you are interested in postdoctoral research positions or collaborative research opportunities. Thank you for your interest in the NIST Ceramics Division.

Debra L. Kaiser
Chief, Ceramics Division

Technical Highlights

The Technical Highlights section of this Report comprises six examples of the exciting outputs of the Ceramics Division. They are:

- Ultra-Small-Angle X-ray Scattering (USAXS) Imaging of Human and Artificial Tissues
- Data Evaluation Theory and Practice
- Inorganic Crystal Structure Database: Accessibility in Support of Materials Research and Design
- Crystal Chemistry of Novel Wireless Dielectrics: Bi-Zn-Nb-O Pyrochlores
- Biaxial Stress Dependence of Raman and Photoluminescence Lines in $Al_xGa_{1-x}As$
- Nanoscale Measurement of the Amount of Complex Hydrocarbon Molecules on Magnetic Hard Disks

Ultra-Small-Angle X-ray Scattering (USAXS) Imaging of Human and Artificial Tissues

Just as three-dimensional (3D) imaging has revolutionized clinical medicine, microscale 3D imaging of human and artificial tissues will substantially improve our microstructural understanding of these materials and potentially enable us to develop useful man-made biomaterials. The ultimate goal of tissue engineering is to coax cells into regenerating missing or damaged tissue such as bones or cartilage. This research focuses on obtaining high-contrast real-space images and statistical measures of the microstructures of both of these classes of materials.

Gabrielle G. Long and Lyle E. Levine

Ultra-small-angle x-ray scattering (USAXS) imaging is a high-contrast x-ray technique — developed by MSEL scientists — that provides three-dimensional (3D) microstructural information that is unobtainable using conventional x-ray imaging methods. While the intensity of small-angle scattering as a function of angle provides a measure of the sizes, shapes, and number distributions of the scattering objects, it does not tell us how the scattering objects are arranged. USAXS imaging provides direct information on how the scattering objects are distributed in space, and, thus, can serve as a guide for selected-volume USAXS measurements. Together, USAXS imaging and USAXS data analysis deliver complementary information on the sizes, size distributions and morphology of the microstructures, and how they are arranged in the material. The goal of this research is the nondestructive observation of critical structures responsible for the properties of natural and man-made tissues. This Highlight describes our most recent results from USAXS imaging and USAXS data analysis on human ankle cartilage and man-made tissue scaffolds.

USAXS imaging greatly expands the usefulness of conventional small-angle scattering in four ways. First, it provides direct images of the shapes and 3D arrangements of the scattering objects. Second, the local scattering intensity can be measured as a function of scattering vector, q (where $q = (4\pi/\lambda) \sin\theta$, λ is the x-ray wavelength, and 2θ is the angle of scatter), by comparing images produced at different q values. Third, USAXS imaging greatly extends the size range over which spatial information is obtained. Our USAXS instrument can explore real-space structures from about 1 nm to over 1 μm in size. USAXS imaging extends this range to mm-sized structures. Fourth, USAXS imaging can identify the source of observed scattering. Since the *only* x-rays that contribute to the image are those produced by small-angle scattering, the image is a direct map of the origin of USAXS within the sample.

USAXS images are produced by angle-filtering the x-rays scattered by density variations within a sample, thus providing exceptionally high contrast. While USAXS imaging can provide contrast in cases where radiography and phase–contrast imaging are unsuccessful, the images produced at different scattering angles also may highlight different microstructural features within the same volume, thus providing additional capabilities for exploring complex microstructures.

Our USAXS instrument is located on the UNICAT Sector 33 insertion device beam line at the Advanced Photon Source at Argonne National Laboratory. A pair of silicon {111} crystals selects the energy of the x-rays impinging on the sample, and a pair of mirrors removes higher-order harmonics. Another pair of silicon {111} crystals analyzes the scattered intensity. While the instrument can measure intensities on both sides of the diffraction peak as well as at the peak itself, the USAXS data typically begins 2 to 6 decades below the peak intensity of the transmitted beam and often extends over 8 decades of intensity.

In USAXS imaging, the analyzer crystal pair is rotated to a specific angle and the angle-filtered x-rays form an image of the sample. Since the image contrast does not change during sample rotations about the scattering vector (vertical axis in the lab), we produce stereo USAXS images by combining images from two such rotations. In addition, we have measured 3D rotation series in preparation for full tomographic reconstruction.

USAXS imaging and USAXS scans were made of human ankle cartilage mounted in a wet cell to forestall dehydration. The images that were taken with the scattering vector parallel to the surface of the cartilage showed few structures while images taken with the scattering vector perpendicular to the surface showed copious structures both near the surface (where the collagen fibers are thought to be parallel to the surface) and on the opposite side near the bone (where the collagen fibers are expected to be perpendicular to the bone). The middle of the sample (where the collagen is “disordered”) showed few distinct structures.

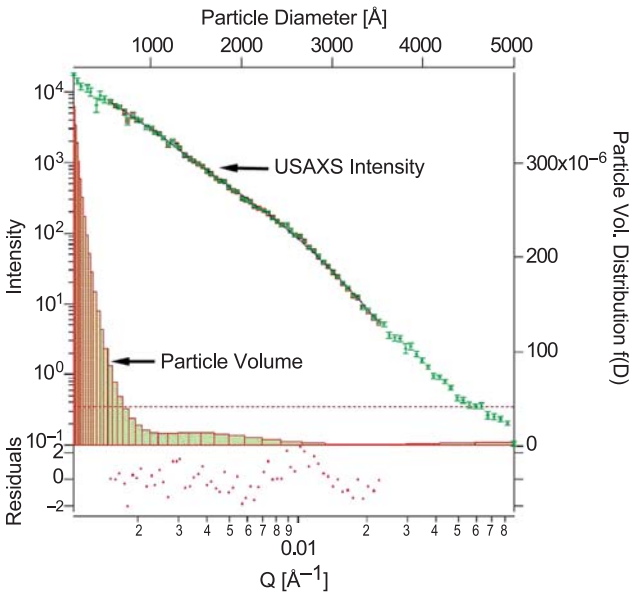

Figure 1: *USAXS data and analysis of the surface region of the cartilage.*

USAXS data and analysis of the surface region, for the scattering vector perpendicular to the surface, are shown in Figure 1. The data were fitted by a broad distribution of spheroids of aspect ratio equal to 5. We find a distribution of sizes starting from the smallest, with few structures above 1000 Å in size.

Analysis of the USAXS scans from the middle region of the cartilage indicated the presence of a bimodal size distribution with the 2nd peak around 1200 Å. In addition, there was evidence of a low-angle diffraction peak. Data from the near-bone edge contained a prominent low-angle diffraction peak at the same position indicating the presence of 650 Å spacings. Interestingly, the microstructures derived from the sample with the scattering vector parallel to the surface, and that from the middle region of the sample perpendicular to the scattering vector were very similar. This supports the model of "disorder" in the middle region.

Polymer-based tissue engineering scaffolds were produced from blended, co-extruded binary polymers of polycaprolactone (PCL) and polyethylene oxide (PEO). After annealing, the PEO was dissolved in water, leaving a porous structure of biocompatible PCL with connected pores approximately 100 µm across. This type of structure is ideal for growing tissues, but the degree of crystallinity on the pore surfaces can strongly affect the cell growth. To explore this effect, an additional annealing/cooling step was added to alter the degree of crystallinity. USAXS scans from the tissue scaffolds contained a pronounced peak near $q = 0.035$ Å^{-1} (180 Å) produced by the lamellar structure of the polymer. The density difference between the amorphous phases leads to enhanced scattering from the crystalline regions.

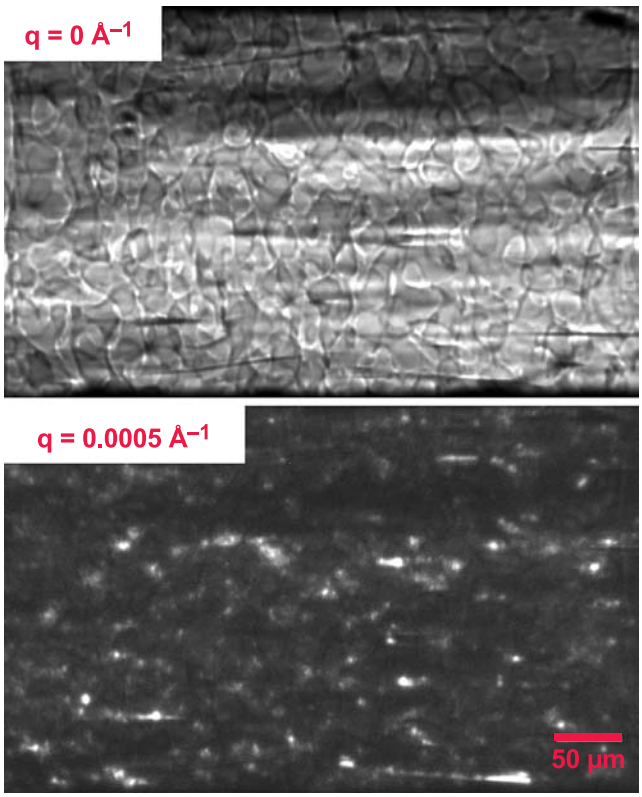

Figure 2: *USAXS images from a slow-cooled tissue engineered scaffold acquired with $q = 0$ Å^{-1} (upper panel) and $q = 5 \times 10^{-4}$ A^{-1} (lower panel).*

Figure 2 shows USAXS images of a slow-cooled tissue scaffold at $q = 0$ Å^{-1} and $q = 0.0005$ Å^{-1}. The upper panel shows the overall pore structure with absorption and phase both contributing to the contrast. Since the scattering at $q = 0.0005$ Å^{-1} is dominated by the crystallites, the image in the lower panel highlights their distribution within the sample. Comparison and superposition of the two images allows us to determine the locations of the crystallites relative to the pore surfaces. Analysis of the scattering curve enables us to extract the crystallite size distribution. The only potential problem in extracting the size distribution is uncertainty over whether double-Bragg diffraction is contaminating the scattering curve. Rotating the sample at $q = 0.0005$ Å^{-1} about the scattering vector shows that the crystallites do not fluctuate in intensity. This proves that the scattering curve is not contaminated by double-Bragg diffraction, and a size-distribution analysis can be made.

For More Information on this Topic

G. Long (Ceramics Division, NIST); C. Muehleman, J. Li (Rush Medical College); T. Irving (Illinois Institute of Technology); J. Dunkers (Polymers Division, NIST)

Data Evaluation Theory and Practice

The rapid pace of technological innovation and the sometimes alarming rate of consumption of natural resources create unprecedented demands to use materials more wisely, more effectively, and more strategically. The availability of reliable data plays a fundamental role in attaining these goals. Ascertaining the credibility of data is the function of data evaluation.

Ronald G. Munro

Credible data form the cornerstone of materials technology. Yet there are relatively few dedicated and sustained efforts to compile and disseminate fully *evaluated* materials property data. The scope of such an undertaking usually is too broad for commercial enterprises and too diffuse for national programs. Consequently, there is a timely and persistent need for guidance on how to assess the reliability of data. Based on more than a decade of research at NIST, the Recommended Practice Guide, *Data Evaluation Theory and Practice for Materials Properties*, SP 960-11 (NIST, 2003), establishes a scientific foundation for data evaluation and provides an extensive range of real-world examples. The Guide examines ***keys*** to assessing data, ***pitfalls*** in applying certain types of property data, and ***criteria*** for consistency among related property values.

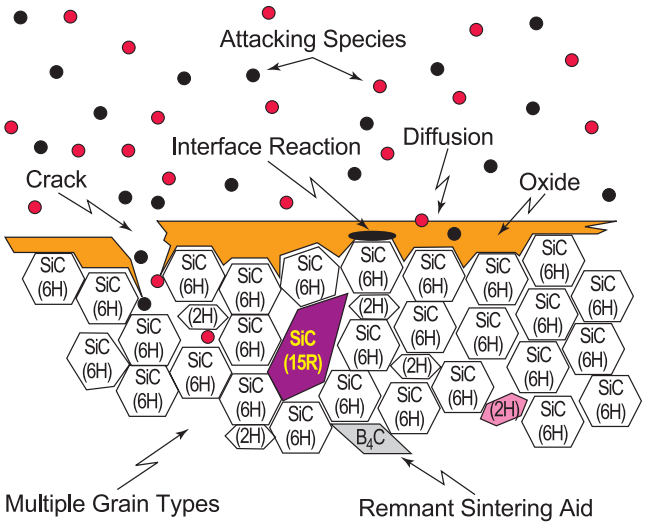

Figure 1: *Data evaluation must account for the complexity of polycrystalline materials and the resulting dependence of material properties on chemical composition, physical microstructure, and environmental conditions.*

Data evaluation is the process by which collections of data are assessed with respect to reliability, completeness, and consistency. As such, data evaluation may be regarded both as a tool and as a formal discipline that plays an intrinsic and an increasingly significant role in advanced technology. Both of these aspects of data evaluation are explored thoroughly in the new NIST Recommended Practice Guide.

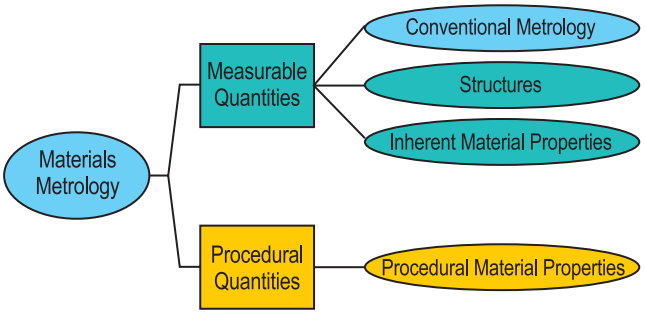

Figure 2: *Formal materials metrology encompasses both the measurable quantities of conventional metrology and a formally new class of quantities known as procedural material properties.*

All design and analytical applications of property data are predicated on the existence of significant collections of property values. Designers need to have values that pertain to the materials that will be used in their products. Materials scientists need values that can be used to distinguish the roles of underlying independent variables and, further, to deduce relations and correlations among properties. Moreover, the development of measurement standards requires data of the highest attainable reliability.

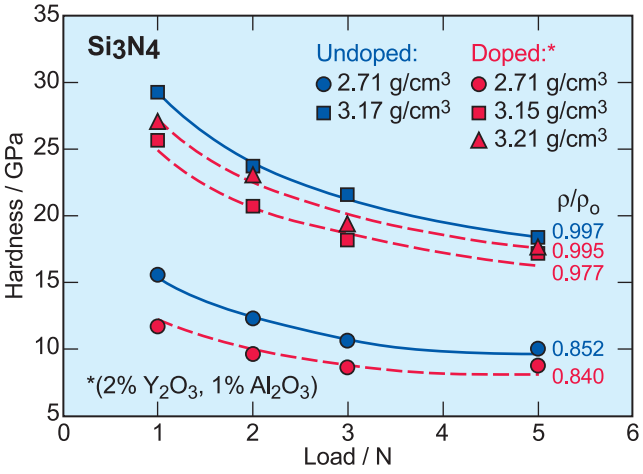

Figure 3: *Measurement results for procedural quantities depend intimately on the measurement details, such as the load applied to the indentor in a hardness test.*

However, it must be recognized that not all useful applications of property data require values of the highest quality. There are relatively primitive, but highly legitimate and abundant, applications of property data that need little more than a rough estimate of a property value. Between the extremes of primitive applications, needing only rough estimates, and advanced designs, relying on fully refined uncertainty analyses, lie a wealth of intermediate requirements that are suitable for diverse purposes. The formal attributes of data evaluation provide the essential means of distinguishing the suitability of data for a given purpose and can do so in the context of the intended application of the data.

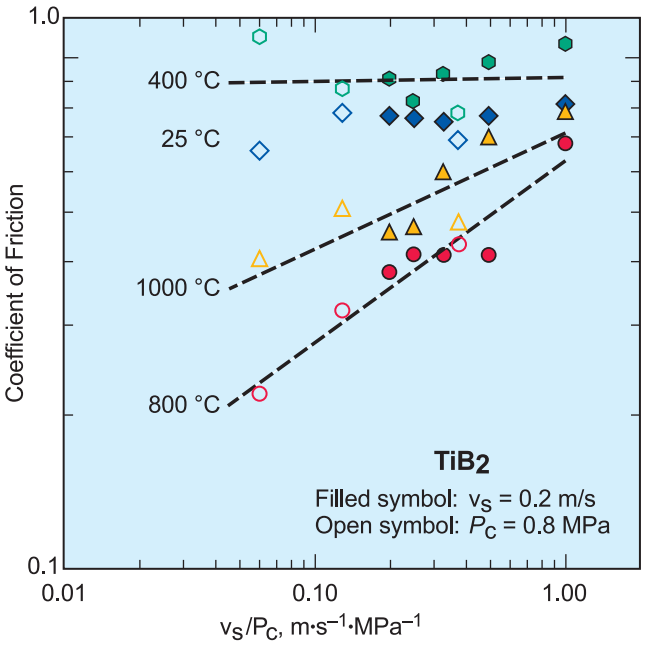

Figure 4: *Empirical correlations often are the first step towards developing physical models or to assessing the limits of validity of proposed mechanisms.*

The Guide, therefore, is directed towards the vast segment of technology whose scientists and engineers must use materials property data, at least on occasion, without the benefit of direct measurement or other assessment experience. The intent is to provide a thoughtful and systematic approach towards establishing confidence in assessing and using collections of numeric materials property data.

To attain this goal, we must first recognize that metrology, like all scientific endeavors, is a paradigm built upon a foundation of concise definitions of basic terms and rational relations. This Guide takes the further view that solutions to common issues that may be encountered with diverse data sources derive from a small number of underlying principles that may be developed generically and applied systematically. Consequently, two chapters of the Guide are devoted to formal considerations: one on materials metrology in general, and one on data evaluation *per se*. Two additional chapters are used to develop and illustrate the practical implementation of the formal principles.

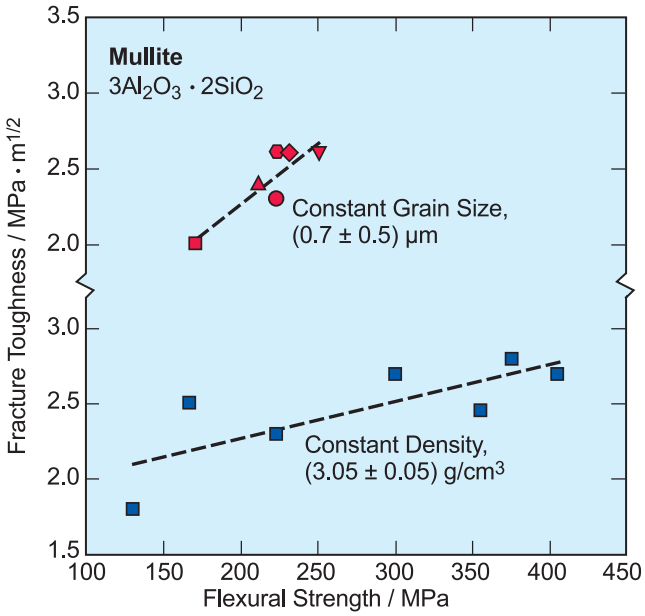

Figure 5: *Models are essential tools in data evaluation helping to identify and understand underlying variables and the roles they play in controlling material behavior.*

The discussions on the theoretical foundations of data evaluation are followed by an extensive collection of examples. All the examples in the Guide are taken from actual exercises in data evaluation, and they are individually selected for the purpose of examining, in succession, the issues of accessibility, reproducibility, consistency, and predictability. Distinctions are made among definitive relations, correlations, derived and semi-empirical relations, heuristic theories, and value estimates. Subtopics include the use of properties as parameters in models, the interpretation of *ad hoc* parameters, and the treatments of procedural properties, response dependent properties, and system dependent data.

For More Information on this Topic

R.G. Munro (Ceramics Division, NIST)

NIST Recommended Practice Guide, *Data Evaluation Theory and Practice for Materials Properties*, SP 960-11 (NIST, 2003).

Inorganic Crystal Structure Database: Accessibility in Support of Materials Research and Design

Access to reliable information on the 3-dimensional structure of crystalline materials helps researchers concentrate experimental work in areas that optimize the discovery process. Researchers and instrument manufacturers have a critical need for evaluated data and also domain specific tools capable of identifying quality structures and compatible data. In cooperation with our partners in the FIZ-Karlsruhe, Germany, NIST has redefined the Inorganic Crystal Structure Database (ICSD) infrastructure, provided expert evaluation of the data, and developed scientific software tools and products. The status and future development are outlined herein.

Vicky Lynn Karen and Alec Belsky

Access to crystal structure data can be a key step in solving research and applications problems involving materials, as in the chemical (catalytic materials), petroleum (zeolites), and electronics (semiconductors) industries. These data are of interest to analysts in areas such as materials design, property prediction, and compound identification. To support these efforts, the ICSD contains three-dimensional crystal structure information for inorganic compounds including ceramics and minerals.

Recent efforts have focused on modernizing and evaluating the ICSD. This has included a complete redesign of the ICSD database structure, conversion and loading of the data into a relational database management system, designing graphical user interfaces to access the data, and creating scientific application modules to analyze the results of a database search. The database system and software design philosophy, Figure 1, used for the ICSD is, in principle,

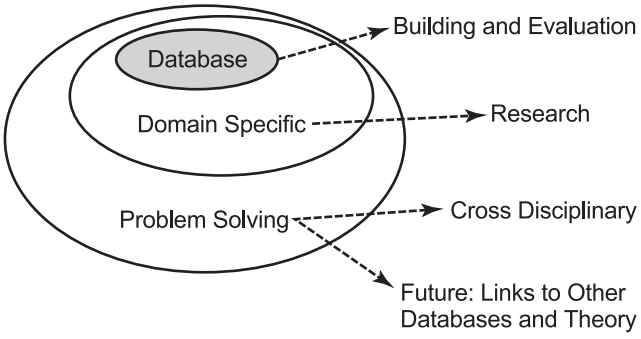

Figure 1: *The idealized model for a distributed database system in materials research and design is composed of 3 layers.*

the same for all materials databases. At the core is a distributed database containing both archival and derived data items. The ICSD graphical user interface represents the intermediate, domain-specific layer, where research and scientific expertise are important. Finally, there is an outer problem-solving layer that cuts across disciplines and links various property databases and theory.

Figure 2: *The latest release of the Inorganic Crystal Structure Database on CDROM.*

The ICSD currently contains more than 65,000 entries. In order to be included in the database, the structure must be fully characterized, the atomic coordinates determined, and the composition fully specified. A typical entry includes the chemical name, formula, unit cell parameters, space group, complete atomic coordinate parameters, site occupation, title, authors, journal or source citation, and other numeric data or metadata, as needed. In addition to the published data, many items are added through expert evaluation and generated by computer programs, such as Wyckoff sequence, molecular formula and molar mass (a.k.a., molecular weight), ANX formula, mineral groups, etc.

Prior to their inclusion in the ICSD, data are examined for completeness and various consistency checks are performed. Several types of evaluation are performed, including examination of individual data for consistency within a complete entry, and determination of the relationship of an individual entry to the entire database.

The first release of the Windows-based product for the Inorganic Crystal Structure Database and a demonstration CDROM was presented at the

XIX Congress and General Assembly of the International Union of Crystallography (Figure 2). Since then, there have been two product updates, adding about 3000 entries and revising the software in response to customer input. The software product is tabular in design and allows for searching in five general categories: Chemistry, Crystal Data, Reduced Cell, Symmetry, and Reference Data. The software includes enhanced features for the characterization of materials based on lattice search and chemistry search modules, and it provides three-dimensional visualization and powder pattern simulation for inorganic structures (Figure 3). The ICSD can be searched in a hierarchy or Boolean mode using NOT, AND, OR logic, and multiple results sets can be generated. The different results sets can be combined and individual entries selected by the user to customize the results for this specific problem. We have provided extensive flexibility for exporting the results into user-defined and standard formats for compatibility with outside applications.

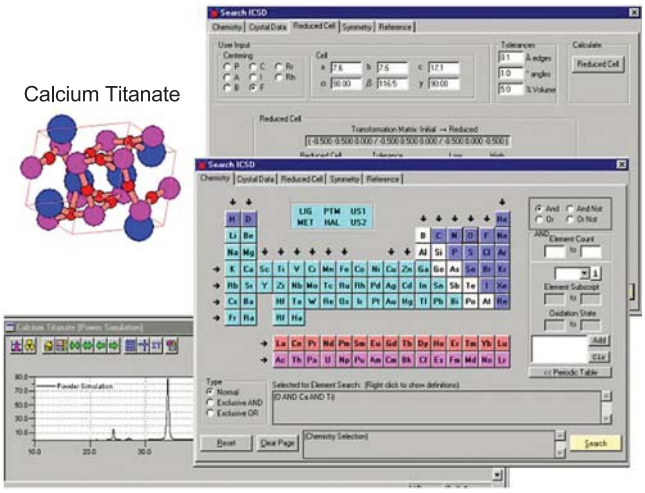

Figure 3: *The new PC graphical user interface for the ICSD is based on a relational database structure.*

The ICSD is directly licensed to private industry, universities, and individual scientists; in addition, there are numerous indirect applications through instrument manufacturers, software vendors, and third party distributors.

In a parallel effort, NIST has two separate data sources containing crystallographic and atomic positional information for metallic crystalline substances, including alloys, intermetallics, and

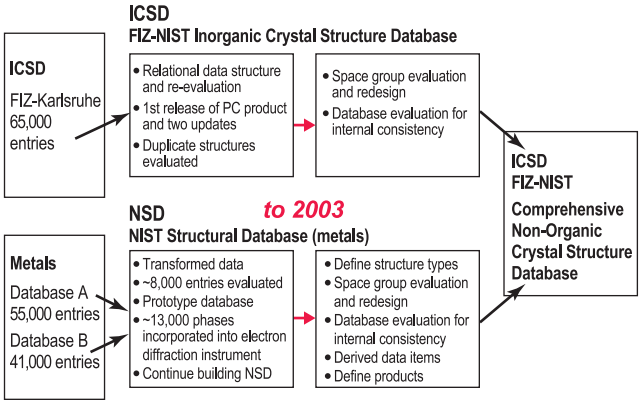

Figure 4: *The development strategy for the ICSD is to establish one comprehensive source of 3-dimensional structure data for all non-organic crystalline materials.*

minerals. Ultimately, our goal (Figure 4) is to combine these data sets with the inorganic data to form a single, comprehensive non-organic crystal database. All entries in the database include three-dimensional structural information with about half having experimentally refined coordinates. It is easy to assume that, because the databases are all crystallographic databases, the process for transforming the Metals and Inorganic data (Figure 4) would be the same. However, this is not the case as widely varying conventions, standards, and formats have been employed throughout all three data sets. For example, expert evaluation is required in order to define and transform even the most critical fields such as chemistry, positions of the atoms, notations for multiple site occupancies, unit cells, and space groups.

In addition to offering one comprehensive source for all non-organic crystalline materials, inorganics, and metals, the interoperability of the ICSD with other data sources is becoming increasingly important for future development. It is our aim that the development strategies and implementations described herein for the ICSD will be compatible with future demands from the materials communities. Planning for this future technology is currently underway.

For More Information on this Topic

V.L. Karen (Ceramics Division, NIST)

NIST Standard Reference Database 84, FIZ/NIST Inorganic Crystal Structure Database (ICSD), **http://www.nist.gov/srd/nist84.htm**.

Crystal Chemistry of Novel Wireless Dielectrics: Bi-Zn-Nb-O Pyrochlores

The primary technology drivers for wireless consumer devices include miniaturization, reduction of component part count, and increased functionality. Multilayer ceramic integrated circuits manufactured using low-temperature co-fired ceramic technology provide a viable solution to this challenge. Recently, bismuth-based pyrochlores have been recognized as attractive candidates for capacitor and high-frequency filter applications in multilayer structures co-fired with metal electrodes. However, understanding of the dielectric behavior of these materials has been impeded by the absence of detailed structural information. In the present study, we conducted a detailed analysis of the cubic pyrochlore-type compound $Bi_{1.5}Zn_{0.92}Nb_{1.5}O_{6.92}$ to establish the details of its crystal chemistry and the structural origin of its dielectric response.

Igor Levin

Ternary oxides in the Bi_2O_3-ZnO-Nb_2O_5 (BZN) system exhibit (Figure 1) high dielectric constants (ε), relatively low dielectric losses, and compositionally tunable temperature coefficients of capacitance (τ_c). Such properties, combined with sintering temperatures of less than 950 °C, render these materials as attractive candidates for capacitor and filter applications in multilayer structures co-fired with silver electrodes. This system features two structurally distinct ternary compounds, $Bi_{1.5}Zn_{0.92}Nb_{1.5}O_{6.92}$ ($\varepsilon \approx 145$, $\tau_c \approx -400\times10^{-6}$/°C) and $Bi_2Zn_{2/3}Nb_{4/3}O_7$ ($\varepsilon \approx 80$, $\tau_c \approx +200\times10^{-6}$/°C), exhibiting very dissimilar dielectric properties. Since the two compounds exhibit opposite signs of τ_c, their mixture yields temperature-compensated ceramics.

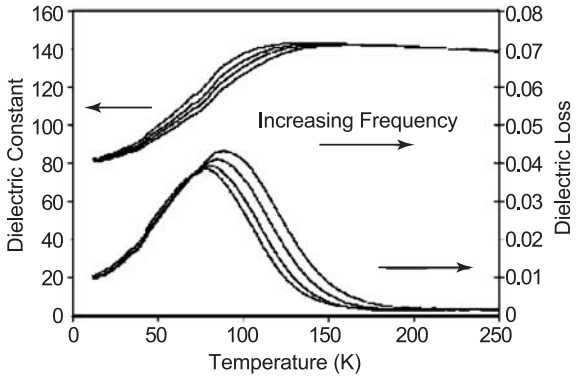

Figure 1: *Dielectric response of pyrochlore-type $Bi_{1.5}Zn_{0.92}Nb_{1.5}O_{6.92}$. (Courtesy of C. Randall and J. Nino, PSU.)*

$Bi_{1.5}Zn_{0.92}Nb_{1.5}O_{6.92}$ ceramics exhibit a low-temperature dielectric relaxation, which has been attributed to a dipolar glass-like mechanism, while no such behavior is observed for $Bi_2Zn_{2/3}Nb_{4/3}O_7$ in the same temperature range.

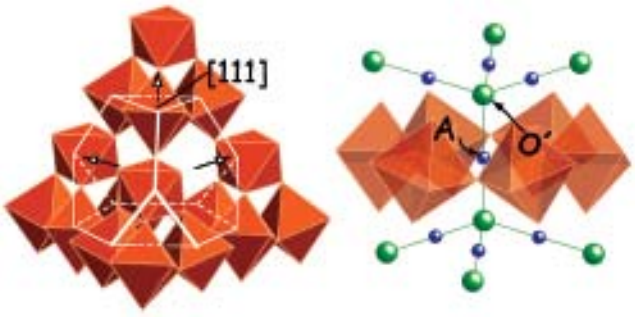

Figure 2: *Illustrations of the pyrochlore structure. Pyrochlores are often described by the formula $B_2O_6{\bullet}A_2O'$, which emphasizes that the structure is built of two interpenetrating networks: $[BO_6]$ octahedra sharing vertices form a three-dimensional network based on a diamond net (left), which results in large cavities occupied by the O′ and A atoms, themselves forming a second cuprite-like A_2O' tetrahedral net (right).*

Despite growing technological interest in these ceramics, their crystal chemistry and the origin of their dielectric behavior have remained uncertain. The compound $Bi_{1.5}Zn_{0.92}Nb_{1.5}O_{6.92}$ was reported to exhibit a cubic pyrochlore structure (Figure 2), $A_2B_2O_7$, implying that the Zn ions occupy both A- and B-sites. However, in the absence of detailed structural/compositional data, the presence of rather small Zn ions on the eight-fold coordinated A-sites remained highly controversial because the ionic radius of Zn falls outside the known limits of structural stability for pyrochlores. The other compound, $Bi_2Zn_{2/3}Nb_{4/3}O_7$, according to our recent work, was found to adopt a monoclinic zirconolite-like arrangement. The zirconolite structure, which, like pyrochlore, can be described as an anion-deficient fluorite-derivative, features a distinctly different type of cation arrangement on the metal sites. In the present work, we conducted a detailed structural analysis of the cubic pyrochlore $Bi_{1.5}Zn_{0.92}Nb_{1.5}O_{6.92}$ to elucidate its crystal chemistry and the origin of the dielectric relaxation.

Electron diffraction patterns from single grains of $Bi_{1.5}Zn_{0.92}Nb_{1.5}O_{6.92}$ were consistent with both a pyrochlore-type unit cell and symmetry. However, several reflections (*e.g.*, 442) observed in the experimental electron, x-ray, and neutron powder diffraction patterns, although accountable by the

Fd3m symmetry, violated special reflection conditions for the 8*b*, 16*c*, 16*d*, and 48*f* sites occupied in the ideal arrangement; these observations suggested that some of the atoms are displaced to lower symmetry positions. Indeed, Rietveld refinements using neutron data confirmed appreciable distortion of the A-site environment that occurs to accommodate the bonding requirements of the A-cations (Figure 3). This distortion is realized through (i) displacements of both A-cations and O′ anions from their ideal high symmetry positions (16*d*-A, 8*b*-O′), and (ii) local tilting of [BO_6] octahedra. A combination of the best fit and most reasonable values of displacement parameters were obtained by placing both A and O′ ions on the 96*g* (*x,x,z*) positions. Similar positional parameters were obtained at both 298 K and 12 K, suggesting that the displacements are static in nature. In the disordered model, each A cation is randomly distributed over six sites, which are displaced from the ideal 16c positions approximately along the three <112> directions perpendicular to the corresponding O′-A-O′ link. The displacements of the A-cations are confined to the {111} layers and result in shortening of three-out-of-six A-O bonds. The displacements of O′ ions occur along all six <110> directions, so that each O′ ion is statistically distributed over 12 sites.

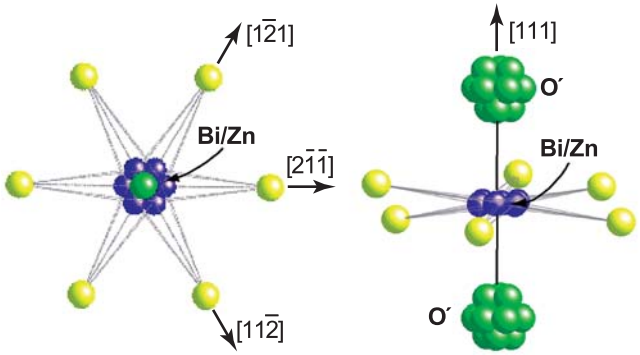

Figure 3: *Nearest-neighbor environment indicated by the refinement results for the A = (Bi/Zn) cations in the BZN pyrochlore. Yellow and green spheres represent O and O′ atoms, respectively, while blue spheres correspond to the A-cations. Left: View along <111> direction with six-randomly occupied A-cation positions indicated by blue spheres. The O′ atoms are shown in the ideal positions for clarity. Right: View along the direction nearly perpendicular to the <111>. The displaced positions of both the A- and O′ atoms are indicated.*

The bond strain about the A-sites is minimized when both O′ ions in the O′-A-O′ link move toward the corresponding {111} layer; these A-sites are expected to be occupied by Zn. Three other O′-A bonds for the same O′ ion will be stretched so that those A-sites are likely to be occupied by Bi. Because no superstructure reflections were observed, any such structural correlation must be short-range in nature. Crystal-chemical considerations suggest local ordering in which each O′ ion is bonded to three Bi and one Zn cations; in such configurations, the bonding requirements of both Zn and Bi can be met. Electron diffraction patterns (Figure 4) revealed weak, yet well-structured, diffuse scattering which can be attributed to such short-range ordering of Bi and Zn on the A-sites.

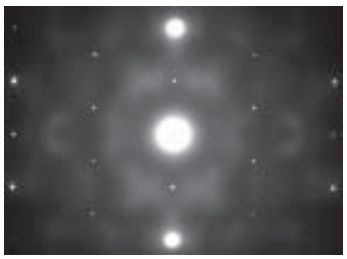

Figure 4: *High-index zone axis electron diffraction pattern from the pyrochlore $Bi_{1.5}Zn_{0.92}Nb_{1.5}O_{6.92}$ reveals well-structured diffuse scattering likely associated with local ordering of Bi and Zn.*

Studies of $Bi_{1.5}Zn_{0.92}Nb_{1.5}O_{6.92}$ using far-infrared spectroscopy, conducted by S. Kamba at the Institute of Physics in Prague, indicated that the lowest frequency O′-A-O′ bending mode provides the strongest contribution to the dielectric constant while the contribution of the O-A-O bending is also significant. Both types of bending resemble those produced by the presently identified static displacements of the A, O′ and O atoms; therefore, these displacements are expected to have a strong effect on the dielectric response of the cubic pyrochlore-type compound. Thus, the displacive disorder in the A_2O' network most likely is the origin of the "glass-like" dielectric behavior observed for $Bi_{1.5}Zn_{0.92}Nb_{1.5}O_{6.92}$.

These studies of cubic pyrochlore-type $Bi_{1.5}Zn_{0.92}Nb_{1.5}O_{6.92}$ have established a new crystal–chemical mechanism for the accommodation of small cations such as Zn on the A-sites of the pyrochlore. This new principle has been applied to interpret the structural behavior of other new pyrochlore compounds in the Ca-Ti-Nb-O and Ca-Ti-Ta-O systems. These phases were found to contain a mixture of Ca and Ti on the A-sites, disordered displacements of Ti and O′ atoms, and, also, dielectric relaxation similar to that observed for the cubic Bi-Zn-Nb-O pyrochlore.

For More Information on this Topic

Igor Levin (Ceramics Division, NIST)

I. Levin, T.J. Amos, J.C. Nino, T.A. Vanderah, C.A. Randall, and M.E. Lanagan. "Structural Study of an Unusual Cubic Pyrochlore $Bi_{1.5}Zn_{0.92}Nb_{1.5}O_{6.92}$." *J. Solid State Chem.*, **168** [1], 69–75 (2002).

I. Levin, T.J. Amos, J.C. Nino, T.A. Vanderah, C.A. Randall, M.E. Lanagan, and I.M. Reaney. "Crystal Structure of Compound $Bi_2Zn_{2/3}Nb_{4/3}O_3$." *J. Mater. Res.*, **17**(6), 1406–1411 (2002).

Biaxial Stress Dependence of Raman and Photoluminescence Lines in $Al_xGa_{1-x}As$

Device manufacturers in the optoelectronics and microelectronics industries have expressed the need for a measurement technique to evaluate local residual stresses in thin film systems. In response, this project seeks to calibrate biaxial stress-induced peak shifts in the first order Raman and photoluminescence (PL) lines of $Al_xGa_{1-x}As$ as functions of both stress and composition (x) to provide a set of tools that can simultaneously determine composition and biaxial stress state. While the calibrations are specific to $Al_xGa_{1-x}As$, the approach is expected to be generally applicable to other semiconductor systems.

Grady S. White and Albert J. Paul

Layered structures of ternary semiconductor compounds, *e.g.*, $Al_xGa_{1-x}As$, are routinely used in optoelectronics as light sources and detectors. The wavelengths at which these devices perform, as well as their mechanical and electronic stability, are functions of the stress (strain) under which they operate. Similar semiconductor ternary compounds are used in the microelectronics industry and are subject to the same stress-driven effects. The stresses, generated during processing, are inherent in the devices and are normally predicted by design models. However, there is currently no way for the accuracy of the models to be confirmed experimentally. The goal of this project is to develop a suite of tools, consistent with those used in industry, that can measure local stresses for model verification.

Photoluminescence (PL) is widely used in the U.S. optoelectronic and microelectronic industries to monitor thin film composition in multilayer devices. Because the same instrumentation can be used for both PL and Raman measurements and because Raman peak positions are known to be stress sensitive, these two techniques were chosen as developmental probes for simultaneously monitoring film stress and composition. The critical question addressed is whether a combination of the two techniques allows separation of stress-induced peak shifts from composition-induced peak shifts, thereby allowing simultaneous evaluation of both stress and composition.

For this study, $Al_xGa_{1-x}As$ films with x = 0.2, 0.5, 0.8, and 0.9 were deposited by molecular beam epitaxy on commercial 655 µm thick, 75 µm diameter undoped GaAs substrates. The deposition temperature was 600 ± 5 ºC and the film thickness, in each case, was nominally 3 µm. Bulk x = 0 specimens were cleaved from a polished, undoped, GaAs substrate, 500 µm in thickness and 50 mm in diameter. All specimens were oriented with the (100) direction normal to the plane formed by the specimen surface. Squares 11 mm x 11 mm were cleaved from the wafers and placed into a biaxial loading rig in the optical path of a commercial micro-Raman system.

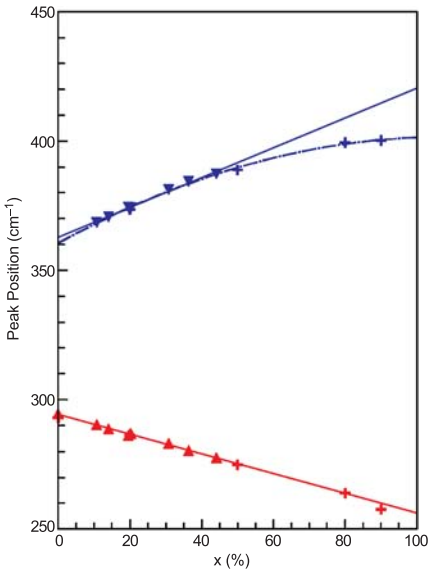

Figure 1: *Unstressed Raman peak positions of GaAs-like (lower) and AlAs-like (upper) peaks as function of x. Triangles and "+" symbols represent two sets of specimens.*

First order Raman spectra of $Al_xGa_{1-x}As$ ($0 < x < 1$) consist of both a GaAs-like line and an AlAs-like line. Figure 1 shows the peak position as a function of x for both of these lines in the absence of stress. The GaAs-like line is linear across the entire composition range, whereas the AlAs-like line is clearly nonlinear and is well described by a quadratic expression ($R^2 > 0.99$).

Data in Figure 2 were obtained from the GaAs-like line of two x = 0.5 specimens. The behavior shown in Figure 2 is typical of the behavior at all compositions for both the GaAs-like and the AlAs-like peaks. Peak shifts are linear with stress, and the peak position decreases with increasing stress. Error bars in all of the figures represent the 95 % Confidence Level.

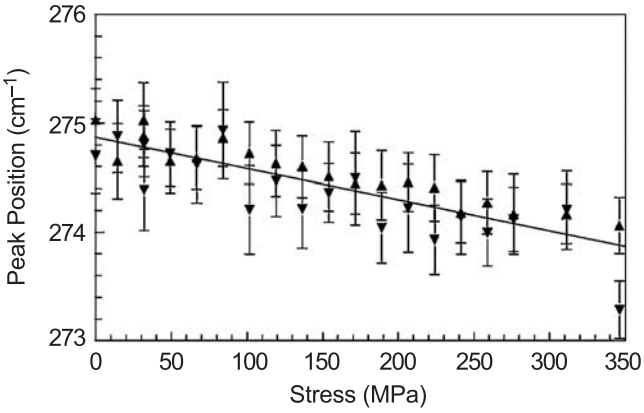

Figure 2: *Peak shift of GaAs-like peak; x = 0.5. The upward and downward triangles represent data taken from two different specimens.*

Figure 3 shows the change in peak position/stress for both Raman lines as a function of composition. Within the precision of the Raman measurements, the stress sensitivity of both lines is independent of x. However, the AlAs-like line shifts almost 50 % more for a given stress than the GaAs-like line. Figures 2 and 3 show that while the phonon energy of both the GaAs-like and the AlAs-like peaks depend strongly upon the relative amounts of Ga and Al in the unit cells, the change in energy with the application of stress is essentially independent of the Ga/Al ratio.

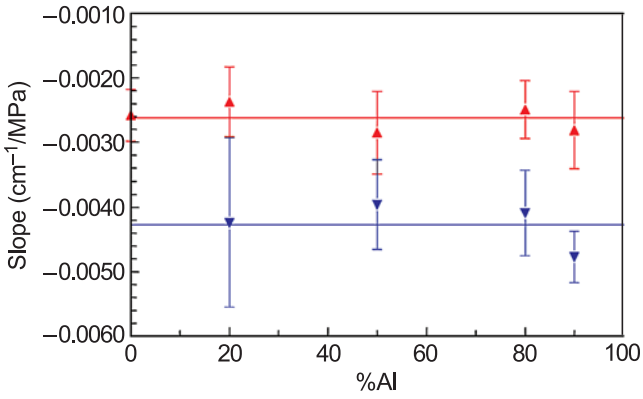

Figure 3: *Slopes (i.e., peak position/stress) of Raman lines as a function of composition: GaAs-like peak (top) and AlAs-like peak (bottom).*

In contrast to the Raman lines, the PL peak shift with stress (Figure 4) shows strong composition dependence for the direct electron transition (x < 0.5). For x = 0.8 and 0.9, the PL spectra are more complicated and result from indirect transitions. The peak positions in this region, while still dependent on x, are essentially independent of stress. The values shown in Figure 4 for x = 0.8 and 0.9 are averages of the multiple peaks composing the PL at those compositions. However, none of the individual peaks deviates substantially from the average values shown in Figure 4. At x = 0.5, the PL is also indirect. However, at that composition, the PL spectrum consists of several peaks that are essentially independent of stress (upper point in Figure 4) and one peak that is stress dependent (lower point in Figure 4).

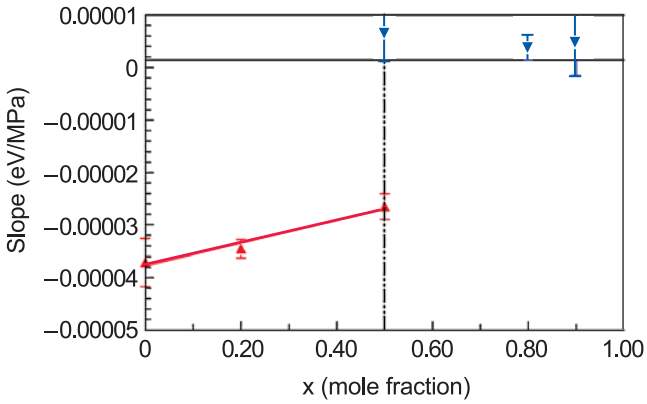

Figure 4: *Slopes (i.e., peak position/stress) of PL lines as a function of composition. In the left side of the figure, PL results from direct transition; in the right side, PL results from indirect transition.*

Because both the Raman and PL spectra are functions of stress and composition, the combination of measurements can be used to solve for composition and biaxial stress state simultaneously. Even for x > 0.5, where the PL is independent of stress, the measured composition dependence of the PL lines coupled with the stress and composition dependence of the Raman lines permits both composition and stress to be determined. Because both the GaAs-like and the AlAs-like Raman line positions have been calibrated for both stress and composition, there are three, rather than two, peaks that provide information regarding stress and composition. The existence of the third peak provides a tool for self-consistency checks on the values obtained.

A manuscript, *Biaxial Stress Dependence of the GaAs-Like and AlAs-Like Raman Lines in $Al_xGa_{1-x}As$,* by G.S. White, A.J. Paul, K.A. Bertness, and A. Roshko that describes the Raman measurements in detail, has been submitted for publication.

For More Information on this Topic

G.S. White, A.J. Paul (Ceramics Division, NIST); K.A. Bertness, A. Roshko (Optoelectronics Division, NIST)

Nanoscale Measurement of the Amount of Complex Hydrocarbon Molecules on Magnetic Hard Disks

The requirement for protection in the head-disk interface is rising. In order to reach 1 Terabit/in^2 areal density and double the data transfer rate, the spacing between the head and disk is shrinking to 3.5 nm at a flying speed approaching 40 m/s. Occasional contacts will test the shear strength of the molecular layer on top of the carbon overcoat. Current lubricant molecules are alcohol-functionalized perfluoropolyether which are inert and oxidatively resistant but lack solubility and surface bonding strength. Alternative molecules such as multiply alkylated cyclopentanes are being considered to improve protection. In order for any alternate molecules to be used, the average molecular thickness on a hard disk surface needs to be measured accurately at 10Å ± 1Å. We have developed a unique master calibration technique that, for the first time, is able to accurately determine the average molecular thickness of a complex hydrocarbon mixture on magnetic hard disks.

Richard Gates, Charles Ying, and Stephen Hsu

The Information Storage Industry Consortium (INSIC) has set a goal of reaching 1Tbit/in^2 areal density by 2006 with a concurrent increase in data transfer rate approaching 100 Gbit/s. This translates to an extraordinarily ambitious technical goal of a 10-fold increase in capacity in four years. To reach that goal, the flight height and the carbon overcoat thickness need to be reduced to 3.5 nm and 1 nm respectively. Since the disk is protected by the thickness of the carbon overcoat and 10Å of lubricant molecules, alternative carbons and lubricant molecules are needed to provide the same degree of protection with one-fifth the amount of lubricant and overcoat.

Under the proposed new design, head-disk interface contacts are inevitable due to reduced flight height, waviness of the disk, and rotational wobble. One of the key characteristics that has been identified for protective molecules is the adhesive strength to resist high shearing action. A typical solution in this case would be to add strongly surface-bonding molecules to the lubricant as additives. The current disk lubricant, a functionalized perfluoroalkyl ether, has limited solubility. Therefore, hydrocarbon molecules with extremely low volatility characteristics are needed. Multiply alkylated cyclopentane is one such molecule.

Current industrial practice of measuring the thickness of perfluoroalkyl ether on a hard disk surface (tip to valley distance from 15 Å to 25 Å) relies on a cross calibration between fourier transform infrared spectroscopy (FTIR) and x-ray photoelectron spectroscopy (XPS) on CF2 bonds which is symmetrical and sharp. For complex hydrocarbons, there are multiple peaks interrelated at different frequencies, and there is no established technique for such measurement.

The measurement of "average film thickness" needs to be defined. The lubricant molecules are a complex mixture of isomers with different molecular weights. The surface is atomically rough, and the coverage is below the full "monolayer" level. Nano- and microscale aggregations undoubtedly take place, and the distribution of molecules across the surface hills and valleys is not known. Recent data from UC Davis tend to support this observation. High-frequency modulation atomic force microscopy (AFM) was used to image the surface, and from these data, elasticity information can be extracted. Figure 1 relates the topographic image with elasticity of a hydrocarbon covered hard disk surface. The bottoms of the valleys show higher hardness suggesting that the hydrocarbon molecules do not reside at the bottom of the valleys.

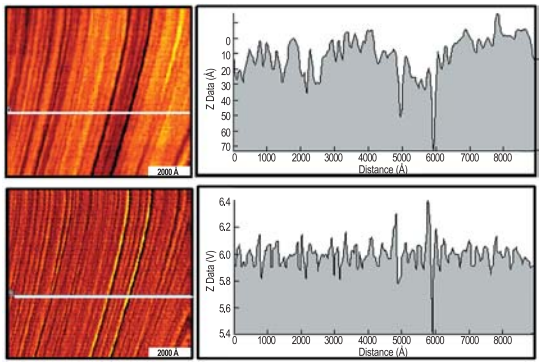

Figure 1: *AFM topographic images and elasticity data.*

Detection and measurement of a one nanometer thick complex molecular layer on a rough surface taxes the detection limits of analytical instrumentation. We first used FTIR and a modified XPS technique. The modified XPS technique scanned the surface twice: once without lubricant coverage and once with lubricant coverage. The decrease of x-ray photoelectron signal intensity from the molecule coverage was used to estimate film thickness. Unfortunately, the carbon overcoat thickness was found to vary along the radial direction of the disk. Depending on the specific batch of disks tested, the variation could be as much as 5 %–10 % from the inside radius to the outer edge of the disk. Hence, this measurement technique is insufficient to measure the "molecular thickness" as required by industry to control the process.

We tried various techniques such as AFM scratching, ellipsometry, and x-ray reflectivity (XRR). The latter technique has difficulty with surface roughness and the fact that the average film thickness is below the peak-to-valley distance. For AFM, the molecules wet the tip. Ellipsometry data at this range have large scatter. So the conclusion is there is no acceptable technique to measure such "film thickness" of a complex hydrocarbon molecular mixture to the industrial specification of 10 Å ± 1 Å.

To develop a solution to this industrially important issue, we created a master calibration sample approach. Basically we deposit a known (gravimetrically) solution on a disk with a barrier film surrounding a known area and allow the solvent to evaporate under controlled conditions. The resulting "film thickness" can then be used to calibrate various instruments. The challenges are uniform distribution of molecules across the area, containment of fluid, meniscus forces, and evaporation rate control.

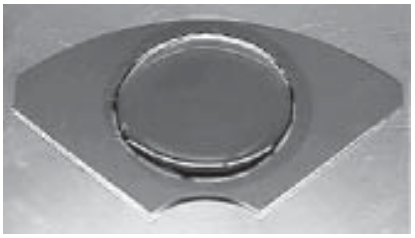

Figure 2: *Confined lubricant solution on a hard disk.*

Initially, this approach was attempted with liquid–phase samples; however, under these conditions, evaporation and meniscus forces lead to uncontrolled lubricant film uniformity. This was solved by evaporating the solvent from the mixture while it is in the solid state. The solution is placed within the barrier (Figure 2) and rapidly frozen using liquid nitrogen. Then the solvent is slowly removed by evaporation into an inert gas at –10 °C.

By controlled slow evaporation of solvent directly from a solid frozen state, we avoid the meniscus and surface tension forces which tend to create non-uniformity of the liquid mass. A pseudo "sublimation" process is created. In this way, uniform signal detection by FTIR confirms that the distribution of molecules across the area is less than 5 % at less than full monolayer coverage. Using this new technique, a series of "film thickness calibration standards" was created (see Figure 3).

A series of three master calibration samples was prepared and submitted for XPS photoelectron attenuation analysis. The very small variation of XPS intensity across the disk surface indicated that film uniformity was quite good, varying by less than 5 %. A correlation plot of XPS estimated thickness versus master calibration target thickness (Figure 4) yielded a straight line, but the slope was not 1.0 (referenced in red). This indicates that the XPS attenuation technique has an inherent bias due to inaccurate assumptions in the model used in the analysis. The observation that the slope of the XPS versus target thickness correlation is 0.6 indicates that the initial XPS attenuation technique was underestimating the hydrocarbon film thickness by about 40 %. The effect has been attributed to the difference in density between the hydrocarbon and carbon overcoat. Utilizing this information, the model was refined to accommodate this effect.

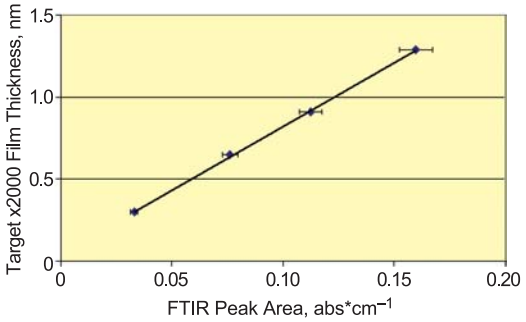

Figure 3: *Calibration curve relating FTIR signal to known hydrocarbon film thickness determined gravimetrically. Error bars are one standard deviation.*

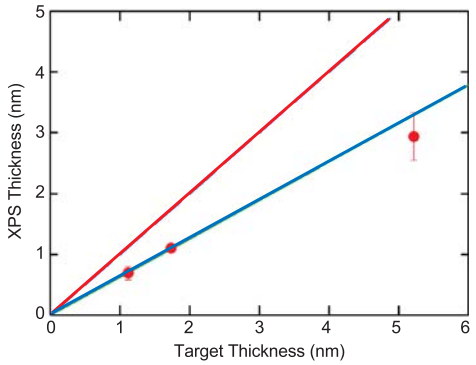

Figure 4: *XPS signal calibration for known hydrocarbon film thickness. Error bars are one standard deviation.*

A calibration method for nanometer-scale complex hydrocarbon films on an engineering surface has been developed. The method is based on gravimetric solution preparations and utilizes a novel freeze-evaporation technique to extract the carrier solvent while leaving a uniform film of complex hydrocarbon on the surface. The method can be applied to a variety of surfaces and offers the potential for calibrating many different analytical techniques for their ability to measure thickness of complex hydrocarbons.

For More Information on this Topic

S. Hsu (Ceramics Division, NIST)

Combinatorial Methods

The Combinatorial Methods Program develops novel high-throughput measurement techniques and combinatorial experimental strategies specifically geared towards materials research. These tools enable the industrial and research communities to rapidly acquire and analyze physical and chemical data, thereby accelerating the pace of materials discovery and knowledge generation. By providing measurement infrastructure, standards, and protocols, and by expanding existing capabilities relevant to combinatorial approaches, the Combinatorial Methods Program lowers barriers to the widespread industrial implementation of this new R&D paradigm.

The Combinatorial Methods Program has adopted a two-pronged strategy for accelerating the development and implementation of combinatorial approaches: an active intramural R&D program and an ambitious outreach activity. The intramural R&D program is designed to better tailor combinatorial methods for the materials sciences and extend the state-of-the-art in combinatorial techniques. Measurement tools and techniques are developed to prepare and characterize combinatorial materials libraries, often by utilizing miniaturization, parallel experimentation, and a high degree of automation. A key concern in this effort is the validation of these new approaches with respect to traditional "one at a time" experimental strategies. Accordingly, demonstrations of the applicability of combinatorial methods to materials research problems provide the scientific credibility needed to engender wider acceptance of these techniques in the industrial and academic sectors. The successful adoption of the combinatorial approach also requires a highly developed "workflow" scheme. All aspects of combinatorial research, from sample "library" design and library preparation to high-throughput assay and analysis, must be integrated through an informatics framework, which enables iterative refinement of measurements and experimental aims. Combinatorial Methods Program research projects give illustrations of how combinatorial methodology is implemented effectively in a research setting.

NIST-wide research collaborations, facilitated by the Combinatorial Methods Program, have produced a wide range of new proficiencies in combinatorial techniques, which are detailed in a brochure, "Combinatorial Methods at NIST" (NISTIR 6730), and online at www.nist.gov/combi. Within the Materials Science and Engineering Laboratory (MSEL), novel methods for combinatorial library preparation are designed to encompass variations of diverse physical and chemical properties, such as composition, film thickness, processing temperature, surface energy, chemical functionality, UV-exposure, and topographic patterning of organic and inorganic materials ranging from polymers to nanocomposites to ceramics to metals. New instrumentation and techniques have been developed that enable the high-throughput measurements of adhesion, mechanical properties, failure mechanisms, film thicknesses, and refractive index, among others. The combinatorial effort extends to multiphase, electronic, optoelectronic, and magnetic materials, including biomaterials assays. On-line data analysis tools, process control methodology, and data archival methods are also being developed as part of the Program's informatics effort.

The extensive outreach activity in the Combinatorial Methods Program is designed to facilitate technology transfer with institutions interested in acquiring combinatorial capabilities. The centerpiece of this effort is the NIST Combinatorial Methods Center (NCMC), an industry–university–government consortium organized by MSEL that became operational on January 23, 2002 via a kick-off meeting in San Diego. The recognized importance of NCMC activities is readily apparent, as 15 industrial partners, the Air Force Research Lab, and the University of Southern Mississippi are participating in the NCMC membership program. The membership continues to grow and 80 % of the members from last fiscal year have already renewed for this fiscal year. The NCMC facilitates direct interaction between NIST staff and these industrial partners, and it provides a conduit by which Combinatorial Methods Program research products, best practices and protocols, instrument schematics and specifications, and other combinatorial-related information can be effectively disseminated. This outreach is mediated in large part by a series of semi-annual workshops for NCMC members. Indeed, since its inception, four NCMC workshops have been held at NIST. Further information on the NCMC can be found on the website at www.nist.gov/combi.

Contact: Peter K. Schenck

Combinatorial Tools for Materials Science

Combinatorial methods are increasingly used by industry for the discovery and optimization of materials for use in electronic, optical, and magnetic applications as well as for designing chemical and biological sensors and for creating molecular patterns. We have developed tools for the fabrication of thin film libraries and characterization of thickness and optical properties. We introduce combinatorial near edge x-ray absorption fine structure as a new tool for the rapid, non-destructive determination of the chemistry (including bond concentration) and molecular orientation of chemically heterogeneous surfaces.

Peter K. Schenck and Daniel A. Fischer

We have developed combinatorial tools that can be applied to a broad range of materials: a pulsed laser deposition (PLD) system for thin film library fabrication; a rapid throughput, spatially-resolved spectroscopic reflectometer for mapping thickness and refractive index; and a combinatorial near edge x-ray absorption fine structure (NEXAFS) tool.

PLD is a versatile, rapid method for growing thin films that has the following advantages: complex target compositions are possible; congruent vaporization leads to stoichiometric material transfer; high energy process; low substrate temperatures; and high deposition rates. Our deposition chamber utilizes a dual-beam, dual-target configuration designed for the fabrication of compositionally graded films. Thickness and optical property assays are performed on the film libraries using a semi-automated spectroscopic reflectometry apparatus.

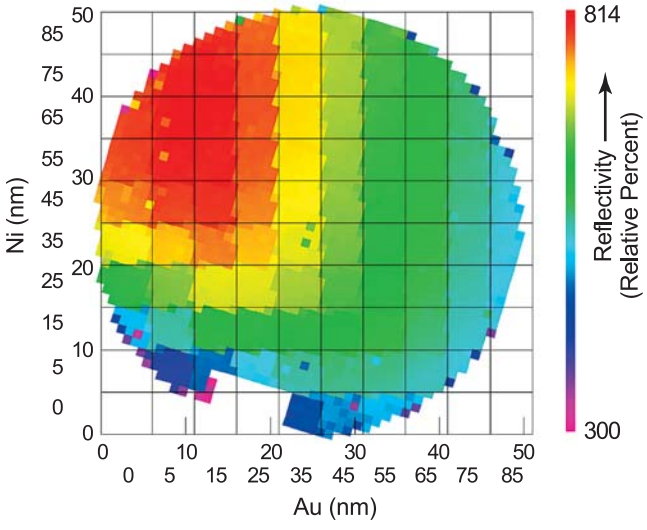

Figure 1: *Reflectivity (450–500 nm, relative to sapphire) of Ni-Au interconnects on GaN after heating to 400 °C.*

$BaTiO_3$-$SrTiO_3$, Au-Ni, and Au-NiO film libraries have been deposited and characterized using these tools. In addition, combinatorial library films of Ni-Au interconnects (88 compositions) on GaN have been characterized before and after annealing (as shown in Figure 1).

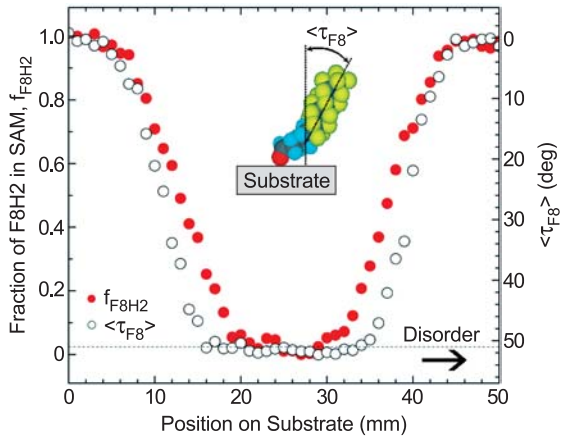

Figure 2: *Fraction of F8H2 in the SAM (f_{F8H2}) (closed circles) and the molecular orientation (open circles).*

Combinatorial NEXAFS is used to simultaneously determine molecular orientation and bond chemistry of planar, chemically heterogeneous surfaces. Information on the chemistry and molecular organization of chemical groups on surfaces is needed, for example, to shed light on the behavior of monomolecular templates and surface modifiers and to characterize new classes of catalysts. We illustrate the power of the combinatorial NEXAFS method by simultaneously probing the concentration and molecular orientation of semifluorinated $F(CF_2)_8(CH_2)_2SiCl_3$ (F8H2) molecules in self-assembled monolayer (SAM) gradients on flat silica substrates as shown in Figure 2.

Notable Outputs: Invited paper in *Chemistry in Britain*, May 2003 (pgs. 45–47), "Blazing a Trail." Cover of *Applied Physics Letters*, January 13, 2003 (pgs. 266–268) and press release, January 17, 2003, Brookhaven National Laboratory, "Scientists Develop Technique to Determine Molecular Structure of Heterogeneous Surfaces."

Contributors and Collaborators

M. Vaudin, J. Kim, J. Blendell (Ceramics Division, NIST); A. Davydov (Metallurgy Division, NIST); E. Bretschneider (Uniroyal Optoelectronics); J. Genzer, K. Efimenko (North Carolina State University)

Data and Data Delivery

The economic importance of technical data has grown steadily over the past three decades. NBS/NIST took an important lead early in the effort to emphasize the pervasive use and increase the impact of reliable materials property data. As early as 1985, former NBS Director E. Ambler noted that the need for property data had become a "national priority," while the National Research Council repeatedly observed that there is a persistent "critical national need" for materials property data.

The NIST Materials Science and Engineering Laboratory (MSEL) has been a prominent leader in responding to this national need. By design, the scope of the MSEL effort is evolutionary and responds to the ever-increasing advances in technology. Currently, MSEL has six project areas in the Data and Data Delivery program.

- ***Crystallographic and Phase Equilibria Databases*** *[Project Leader — V. Karen]:* This project encompasses the two most venerable efforts in MSEL, each of which recently has had a major new release. In collaboration with Fachinformationszentrum Karlsruhe (FIZ, Germany), a CDROM version of the FIZ/NIST Inorganic Crystal Structure Database (ICSD) has been released providing the full structural data, *i.e*., lattice parameters and atomic coordinates, for approximately 60,000 compounds. The long-standing collaboration between NIST and the American Ceramic Society (ACerS) has continued with the completion of a new topical volume in the NIST/ACerS Phase Equilibria Diagrams series, the first of two planned volumes on electronic ceramics.

- ***Phase Equilibria and Properties of Dielectric Ceramics*** *[Project Leader — T. Vanderah]:* An integrated theoretical and experimental effort is underway to predict and measure phase equilibria and electronic behavior in dielectric oxide systems. This work includes relaxor ferroelectrics, dielectrics for cellular infrastructure and hand-held devices, and dielectrics for low temperature co-fired ceramics for applications in multilayer ceramic integrated circuit technology. The impact of this work was evident in Dr. Vanderah's invited perspective article, "Talking Ceramics," which appeared in the journal *Science*. The timeliness of this work was emphasized further by its subsequent feature in the science section of the *New York Times*.

- ***Phase Relationships in High Temperature Superconductors*** *[Project Leader — W. Wong-Ng]:* MSEL's meticulous effort to provide phase information critical to the development of practical superconductors is currently directed towards two important systems: $Ba_2RCu_3O_{7-x}$, where R is yttrium or a lanthanide, and MgB_2. For $Ba_2RCu_3O_{7-x}$, work has focused on the phase relations in BaF_2-BaO-Y_2O_3-CuO_x-H_2O and the interactions of $Ba_2RCu_3O_{6+x}$ with buffer layers, both of which are important for advances in the "BaF_2 *ex situ*" process and the "liquid-phase-epitaxy" process. For MgB_2, the enthalpy of formation, vapor pressure, and sources of variability have been determined.

- ***Reaction Path Analysis in Multicomponent Systems*** *[Project Leader — C. Campbell]:* Many industrial processes rely on multicomponent diffusion to control the formation and dissolution of precipitate phases. MSEL is developing a multicomponent diffusion mobility database for Ni-base superalloys that will be used, for example, to predict the formation of the γ' (ordered FCC) phase during the solidification of superalloys. A workshop, "High Throughput Analysis of Multicomponent Multiphase Diffusion Data," was held in March 2003 to focus on the development of methods to extract diffusion data from multicomponent diffusion couples.

- ***Evaluated Materials Property Data*** *[Project Leader — R. Munro]:* Engineering designs utilizing advanced materials require reliable data. Elasticity, strength, toughness, hardness, creep, thermal expansion, conductivity, diffusivity, and durability are prominent among the data categories needed and desired for materials applications and development. This project is directed both towards the development of evaluated databases of these properties for structural and superconducting ceramics and towards the establishment of the evaluation methodologies that form the foundation of reliable materials property data systems. A significant achievement in this effort is "Data Evaluation Theory and Practice for Materials Properties," SP960-11, the eleventh NIST Recommended Practice Guide produced by MSEL.

- ***Informatics and Visualization in Materials Data Delivery*** *[Project Leader — C. Beauchamp]:* The internet, and the World Wide Web in particular, has become a dominant resource medium for technical information. MSEL has undertaken a major commitment to make its extensive data collections available *via* this medium. New efforts, now underway, will provide web access to the MSEL lead-free solder materials property database and the diffusion data archive that is important for the processing of metal alloys. Additionally, the internet will be used increasingly as a means of disseminating MSEL's prodigious technical publications in the form of electronic manuscripts.

Contact: Ronald G. Munro

Crystallographic and Phase Equilibria Databases

Crystallographic data models are used on a daily basis to visualize, explain and predict the behavior of chemicals and materials, as well as to establish the identity of unknown phases in crystalline materials. Phase diagrams are used throughout the ceramics industry to understand and control the complex phenomena which increasingly underlie advanced industrial material production and materials performance. Literally tens of thousands of structures and phase diagrams have been reported in the literature, all with varying degrees of reliability and completeness. This project develops, maintains, and disseminates comprehensive, critically-evaluated data in printed and modern computerized formats, along with scientific software to exploit the content of these databases.

Vicky Lynn Karen, Terrell A. Vanderah, and Peter K. Schenck

The Inorganic Crystal Structure Database (ICSD) is a comprehensive collection of crystal structures covering the literature from 1915. The ICSD database system now includes chemical and 3-dimensional structure information for more than 65 000 inorganic materials. The data and scientific software are licensed to instrument manufacturers, software vendors, and other third-party distributors as well as to individual researchers in industry and academia. Additional information about the ICSD can be found in the Technical Highlights section of this report.

To service the need for reliable phase diagram data, the NIST Phase Equilibria Data Center and the American Ceramic Society (ACerS) jointly publish a series of critically evaluated collections of phase diagrams. The series "Phase Equilibria Diagrams," originally published under the title "Phase Diagrams for Ceramists" (1964–1992), provides current, evaluated data on the phase equilibria of ceramics and related materials. These publications also provide bibliographic data, graphical representations, and analytical capabilities so that researchers have access to reliable, up-to-date data for use in designing, applying, analyzing, and selecting materials. The published portion of the database includes about 16 000 entries with 26 000 phase diagrams contained in nineteen books and a CD-ROM — over 53 000 units have been sold world-wide. Approximately 1000 new entries are collected from the primary literature each year.

Currently underway is a complete modernization to replace the outdated 1980's system with an integrated production facility using a relational structure that will facilitate electronic publishing in a variety of formats, including a web-based version. Much of this year's effort has involved assisting and working with on-site ACerS staff to design and build the new system, which must incorporate all of the scientific data relationships embodied in the original database.

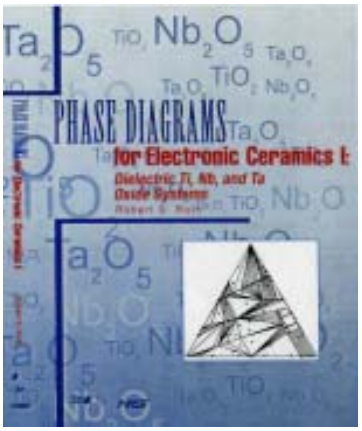

Figure 1: *The latest volume in the series "Phase Equilibria Diagrams" features systems of major interest to the fields of dielectric, ferroelectric, and piezoelectric ceramics.*

The latest database products completed this year include the topical volume, *Phase Diagrams for Electronic Ceramics I: Dielectric Ti, Nb, and Ta Oxide Systems*, edited by R.S. Roth (see Figure 1). This is the first volume of a new collection of phase diagrams focused on the increasingly important field of electronic ceramics. More than 1100 diagrams are presented along with commentaries written by knowledgeable associate editors. Also completed this year was an updated *Cumulative Index 2003* which provides comprehensive indexing of published equilibria data sorted by chemical system and author. In preparation is "Volume XIV — Oxides" (2004) which will contain a wide variety of metal, non-metal, and semi-metal oxide systems — more than 900 entries with 1300 diagrams are already available for inclusion.

Contributors and Collaborators

R.S. Roth, H. Ondik, M.A. Harne (Ceramics Division, NIST); H.F. McMurdie, C. Cedeno, J. You, X. Wang, N. Swanson, E. Farabaugh, M. Mecklenborg (The American Ceramic Society); Fachinformationszentrum Karlsruhe, Germany; D. Watson (Cambridge Crystallographic Data Centre, UK); A. Belsky, S. Young (Measurement Services Division, NIST)

Evaluated Materials Property Data

Reliable data form the cornerstone of materials research and advanced engineering designs. Capturing and assessing materials property data from multiple sources is a key effort in responding to this critical national priority.

Ronald G. Munro

The concurrence of two rapidly advancing technologies, materials science and internet communications, has created the potential for a crisis in the reliability of available materials property information. Once, researchers and designers relied on handbooks and data compilations that were carefully and thoughtfully produced through dedicated and deliberately organized efforts. The magnitude of the effort, the expense, and the time consumed from design to production combined to form an effective quality filter on the results. Efforts not undertaken with a serious and sober intent were strongly deterred by the inevitable costs and commitments.

Now, researchers and designers increasingly turn to the internet for instant access to whatever information is required. The ready accessibility of the internet, however, is as much a weakness as it is a strength. The internet provides a broad open forum where ideas and results can be exchanged and disseminated with remarkable ease, relatively little financial burden, and scarcely any delay between the realization of an idea or result and its expression. Unfortunately, the facility with which information can be conveyed on the internet lacks the inherent process filter that once served as a useful safeguard on the quality of the information content.

The success of the internet in allowing more individuals to communicate more directly and effectively ironically may also cause older information sources to become relatively inaccessible. The materials information populating the internet's information forums represent current efforts. Older information sources, such as handbooks, that have not been adapted to the internet may soon be overlooked or abandoned.

NIST is responding to the full range of challenges presented by these circumstances. The key to reliable data, whether in handbooks or on the internet, is data evaluation. NIST has accepted the responsibility of providing evaluated data on the internet and has taken the lead in educating data users about the methods and significance of data evaluation. Most notably, more than a decade of development and experience in evaluation methodology has been summarized in a new NIST Recommended Practice Guide, SP960-11. (For more information about this Guide, see *Data Evaluation Theory and Practice* in the Technical Highlights section of this report.)

Efforts in the Ceramics Division to provide evaluated data on the internet are focused on the sustained development of the Ceramics WebBook. Currently, three data systems are maintained: Standard Reference Database Number 30, the Structural Ceramics Database (SCD); Standard Reference Database Number 62, High Temperature Superconductors (HTS); and a collection of topical compilations called Property Data Summaries (PDS).

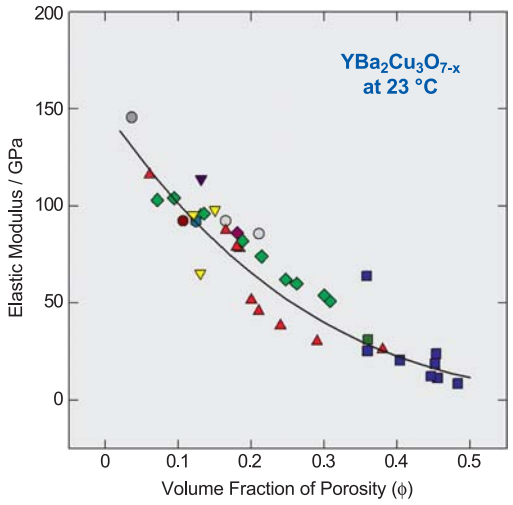

Figure 1: *The elastic (Young's) modulus at room temperature for polycrystalline specimens of the high temperature superconductor Y:123.*

In FY 2003, two additions were made to the Ceramics WebBook. The compilation, *Elastic Moduli Data for Polycrystalline Ceramics*, NISTIR 6853, consisting of approximately 4000 data points, was added to the PDS collection. This collection exhibits the dependence of the elastic moduli (*E, G, B,* ν) on temperature and porosity for approximately 50 ceramic compositions (*e.g.*, Figure 1). A data update was also completed for the Structural Ceramics Database. This update increased the number of citations in the SCD by 100, bringing the total to 834 citations and approximately 38000 data points.

Contributors and Collaborators

C. Sturrock, J. Harris (Ceramics Division, NIST)

Phase Equilibria and Properties of Dielectric Ceramics

Ceramic compounds with exploitable dielectric properties are widely used in technical applications such as actuators, transducers, capacitors, and resonators or filters for microwave communications. The commercial competitiveness of next-generation devices depends on new ceramics with improved properties and/or reduced processing costs. Phase equilibria determination integrated with systematic experimental/theoretical chemistry–structure–property studies contributes toward the fundamental understanding and rational design of these technologically important materials.

Benjamin Burton, Eric Cockayne, Lawrence Cook, Igor Levin, Michael Lufaso, and Terrell Vanderah

Next-generation ceramic packaging requires fabrication of multilayered structures that include embedded functional dielectric ceramics. Technical challenges include understanding and control of deleterious reactions at interfaces during firing. A detailed study of the system Ag-Bi_2O_3-Nb_2O_5-O_2 is in progress to develop a model of interfacial interactions applicable to other co-fired metal–ceramic systems. A partial phase diagram of the system has been determined, and includes a new compound, $Bi_5AgNb_4O_{18}$, which is also observed as a product in $Ag/BiNb_5O_{15}$ reaction couples. Surface diffusion was found to dominate mass transport of Ag at the reaction interface — this phenomenon could be important for co-firing metals with porous ceramics. Further modelling will incorporate kinetic aspects of interfacial reactions using equilibrium thermodynamics as a basis.

Important transducer/actuator materials include Pb-containing perovskite-type relaxor ferroelectrics. First-principles (FP) methods were successfully used to calculate the phonon frequencies for the prototype relaxor $PbMg_{1/3}Nb_{2/3}O_3$. In FP studies of $PbTiO_3$, the dipole moment generated by a nearest-neighbor Pb-O vacancy pair was calculated; the results demonstrate that local electric fields generated by defects strongly affect physical properties. Calculations were also performed for a Pb-free relaxor, $K_{1-x}Li_xTaO_3$. For small x, Li ions are displaced from centrosymmetric positions. The dominant mechanisms for Li hopping between off-centered positions and the resulting effects on the dielectric response were determined.

First-principles methods were also applied to the microwave dielectric system $(1–x)CaAl_{1/2}Nb_{1/2}O_3–xCaTiO_3$. The resulting model yields a dielectric constant that increases with increasing disorder, and increases nonlinearly with increasing x, in agreement with experiment.

Experimental studies of microwave ceramics include structural analyses (by x-ray and neutron powder diffraction) combined with dielectric property correlations of the technically important $Ba_3M^{2+}M^{5+}{}_2O_9$ (M^{2+} = Mg, Zn, Ni; M^{5+} = Nb, Ta) systems. In these systems, the M^{5+} cations tend to undergo a second-order Jahn–Teller distortion and hence shift from the centers of the $[MO_6]$ octahedra — this effect occurs simultaneously with 2:1 B-site cation ordering. Both phenomena influence dielectric response. Modeling of the crystal structures using bond valence methods is in progress to understand the interplay between the distortion and dielectric behavior.

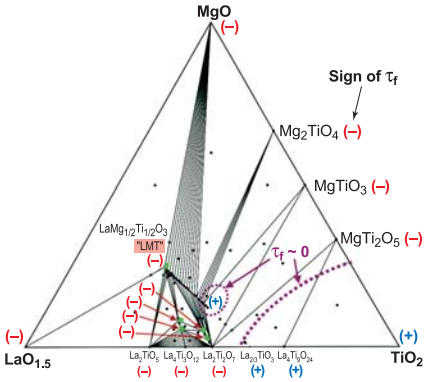

Figure 1: *Subsolidus phase relations in the La_2O_3–MgO–TiO_2 system (air, ≈1450 °C), sign of the temperature coefficient of resonant frequency (τ_f; in parentheses), and approximate locations of two regions of temperature-stable ($\tau_f = 0$) equilibrium mixtures (dotted lines).*

Subsolidus phase equilibria, crystal chemistry, and dielectric behavior were studied for the La_2O_3–MgO–TiO_2 system and for the ternary sections $LaMg_{1/2}Ti_{1/2}O_3$–$CaTiO_3$–La_2O_3 and $LaMg_{1/2}Ti_{1/2}O_3$–$CaTiO_3$–$La_{2/3}TiO_3$. Six phases form in the La_2O_3–MgO–TiO_2 system, and extensive perovskite-type solid solutions form in both ternary sections (see Figure 1). By mapping dielectric properties (relative permittivity and temperature coefficient of resonant frequency, τ_f; 5–10 GHz) onto the phase diagrams, the compositions of temperature-stable ($\tau_f = 0$) compounds and mixtures were predicted. From these studies, it was determined that the quaternary La_2O_3–CaO–MgO–TiO_2 system contains an extensive single-phase, perovskite-type volume through which passes a surface of temperature-stable compositions with relative permittivities in the range of 40 to 50.

Contributors and Collaborators

W. Wong-Ng, R.S. Roth (Ceramics Division, NIST); J.E. Maslar (Process Measurements Division, NIST); R. Geyer (Radio Frequency Technology Division, NIST); S. Bell (TRAK Ceramics, Inc.); K. Leung (Sandia); L. Bellaiche (University of Arkansas); U. Waghmare (JNCASR, India); S. Prosandeev (Rostov State University)

Phase Relationships in High Temperature Superconductors

Phase diagrams serve as "blue prints" for improved processing of high T_c superconductor materials. Of current interest are the $Ba_2RCu_3O_{6+x}$ (R = lanthanides and yttrium) superconductors. The construction of phase diagrams of these systems and the role of phase equilibria and kinetics in the formation of the $Ba_2YCu_3O_{6+x}$ phase using barium fluoride amorphous precursor films are important for rapid advancement of the RABiTS/IBAD coated conductor technology. By providing the phase equilibria data for optimal processing, high T_c technology will be advanced through reductions in cost and improvements in performance.

Winnie Wong-Ng, Lawrence P. Cook, and Igor Levin

In 2003, NIST materials research has continued to provide critical information pertinent to the development of practical superconductors. This project is an integral part of the Department of Energy intensive research program focused on high T_c wires and cables for high-impact commercial applications. Our effort included two principal groups of superconductors: (1) $Ba_2RCu_3O_7$ (Y-213 and R-213, R = lanthanide) coated conductors produced by rolling assisted biaxially textured substrate/ion beam assisted deposition (RABiTS/IBAD); and (2) MgB_2.

Part of our effort has been focused on the dependence of BaO-R_2O_3-CuO_x phase relations (under carbonate-free conditions to match the processing conditions of RABiTS/IBAD conductors) on both oxygen pressure, p_{O2}, and choice of lanthanides. This year, we have completed the study of three systems, with R = Gd, Eu and Ho. The trends of phase formation and tie-line relationships with respect to lanthanide size that were found previously for R = Nd, Sm, Eu, Gd, Ho, Y, and Er, were observed in the present work. Near the BaO-rich region, phase formation was very different from what was found previously for samples prepared in the presence of carbonate.

By mixing the smaller lanthanides R′ with the larger R in the $Ba_{2-x}(R_{1+x-y}R'_y)Cu_3O_{6+z}$ superconductor, both flux-pinning and melting properties can be tailored and optimized. A trend of the extent of solid solution formation with respect to the size of R was observed in $Ba_{2-x}(Nd_{1+x-y}R'_y)Cu_3O_{6+z}$ (R′ = Gd, Y and Yb) and in $Ba_{2-x}(R_{1+x-y}Y_y)Cu_3O_z$ (R = Eu and Gd). There is considerable improvement of critical current density, $J_c(H)$, for samples with partial Y-substitution at high fields at 77 K as compared with that of Nd-213 and Y-213. This improvement is likely due to the increased flux pinning as a result of doping of Nd^{3+} in the Ba^{2+} site.

The "BaF_2 *ex-situ*" process is a promising method for producing long-length, high-quality Y-213 superconducting tapes. Previously, using a controlled-atmosphere differential thermal analysis system, we detected the presence of low temperature liquids in the multicomponent reciprocal Ba-Y-Cu//O,F system, which can be modeled in compositional space as a trigonal prism. This year, we initiated a study to understand the details of complex phase relations in selected Ba-Y-Cu//O,F subsystems: BaO-Y_2O_3-CuO_x-BaF_2, BaF_2-YF_3-CuF_2-CuO_x, BaF_2-Y_2O_3-CuO_x-YF_3, BaF_2-CuO, and BaF_2-Cu_2O. Our results explained the presence of low temperature melts, and confirmed the importance of p_{O2} in oxyfluoride melting reactions.

To control film properties, it is important to understand the details of Y-213 phase evolution from amorphous "BaF_2" films. High temperature x-ray diffraction has been successfully applied to a number of films deposited on $SrTiO_3$ model substrates (provided by Oak Ridge National Laboratory, ORNL). The phase formation sequences in the binary (BaF_2-Y_2O_3, BaF_2-CuO_x and Y_2O_3-CuO_x) and ternary (BaF_2-Y_2O_3-CuO_x) systems have been determined. Further studies of phase evolution of these films on both $SrTiO_3$ and RABiTS substrates will be conducted.

Understanding the interfacial reactions of Y-213 with buffer layers in RABiTS/IBAD films is critical to the development of coated conductor tapes. Since phase diagrams can provide information on how to avoid or control the formation of second phases, we have initiated a study of the BaO-Y_2O_3-CeO_2-CuO_x system (interaction of Y-213 with the CeO_2 buffer layer).

Efforts have continued on the measurement of enthalpy of formation and vapor pressure of MgB_2. Sources of the variability in these properties have also been determined.

Contributors and Collaborators

M. Vaudin (Ceramics Division, NIST); Q. Huang (NIST Center for Neutron Research); R. Shull (Metallurgy Division, NIST); R. Klein (Biotechnology Division, NIST); R. Feenstra (ORNL); T. Holesinger (Los Alamos National Laboratory); M. Rupich (American Superconductor Corp.); J. Kaduk (BP-Amoco); T. Haugan (U.S. Air Force); P. Canfield (Iowa State)

Materials for Micro- and Opto-Electronics

U.S. microelectronics and related industries are in fierce international competition to design and produce smaller, lighter, faster, more functional, and more reliable electronics products more quickly and economically than ever before. At the same time, there has been a revolution in recent years in new materials used in all aspects of microelectronics fabrication.

Since 1994, the NIST Materials Science and Engineering Laboratory (MSEL) has worked closely with the U.S. semiconductor, component, packaging, and assembly industries. These efforts led to the development of an interdivisional MSEL program committed to addressing industry's most pressing materials measurement and standards issues central to the development and utilization of advanced materials and material processes. The vision that accompanies this program — to be the key resource within the Federal Government for materials metrology development for commercial microelectronics manufacturing — may be realized through the following objectives:

- Develop and deliver standard measurements and data;
- Develop and apply *in situ* measurements on materials and material assemblies having micrometer- and submicrometer-scale dimensions;
- Quantify and document the divergence of material properties from their bulk values as dimensions are reduced and interfaces contribute strongly to properties;
- Develop models of small, complex structures to substitute for or provide guidance for experimental measurement techniques; and
- Develop fundamental understanding of materials needed in future micro- and opto-electronics.

With these objectives in mind, the program presently consists of projects led by the Metallurgy, Polymers, Materials Reliability, and Ceramics Divisions that examine and inform industry on key materials-related issues. These projects are conducted in concert with partners from industrial consortia, individual companies, academia, and other government agencies. The program is strongly coupled with other microelectronics programs within government and industry, including the National Semiconductor Metrology Program (NSMP) at NIST. Materials metrology needs are also identified through industry groups and roadmaps, including the International Technology Roadmap for Semiconductors (ITRS), the IPC Lead-free Solder Roadmap, the National Electronics Manufacturing Initiative (NEMI) Roadmap, the Optoelectronics Industry Development Association (OIDA) roadmaps, and the National [Magnetic Data] Storage Industry Consortium (NSIC).

Although there is increasing integration within various branches of microelectronics and optoelectronics, the field can be considered in three main areas. The first, microelectronics, includes needs ranging from integrated circuit fabrication to component packaging to final assembly. MSEL programs address materials metrology needs in each of these areas, including lithographic polymers and electrodeposition of interconnects, electrical, mechanical, and physical property measurement of dielectrics (interlevel, packaging, and wireless applications), and packaging and assembly processes (lead-free solders, solder interconnect design, thermal stress analysis, and co-fired ceramics).

The second major area is optoelectronics, which includes work which often crosses over into electronic and wireless applications. Projects currently address residual stress measurement in optoelectronic films, optical and structural characterization of wide bandgap semiconductors, and standards development for III–V compound semiconductors. Cross-laboratory collaborations with EEEL figure prominently in this work.

The third area is magnetic data storage, where the market potential is vast and growing and the technical challenges extreme. NSIC plans to demonstrate a recording density of 1 terabit per square inch — 40 times today's level — by 2006. To reach these goals, new materials are needed that have smaller grain structures, can be produced as thin films, and can be deposited uniformly and economically. New lubricants are needed to prevent wear as spacing between the disk and head becomes smaller than the mean free path of air molecules. Some measurements require calibration of magnetometers using certified magnetic standards in several different shapes and magnetic strengths, and with a wide range in magnetic character. MSEL is working with the magnetic recording industry to develop measurement tools, modeling software, and standards to help achieve these goals, with MSEL, the Electronics and Electrical Engineering Laboratory, the Physics Laboratory, the Information Technology Laboratory, and the Manufacturing Engineering Laboratory working as partners in this effort.

Contact: Grady White

Nano- and Micro-Electronic Materials Characterization

As the scale of electronic devices is reduced, tools for characterizing materials properties and behavior at the nano- and micro-scale are required. We are developing and characterizing techniques to measure local properties, e.g., texture, strain, chemical homogeneity, and phase evolution, in materials used in nano- and micro-electronic systems.

John E. Blendell and Mark D. Vaudin

The characterization of nano- and micro-electronic materials requires different techniques than those used for bulk electronic materials. For example, optimizing the properties of multilayer systems requires knowledge of the structure and composition of interfaces at nearly atomic resolution. In ferroelectric thin films for ferroelectric random access memory (FRAM), local texture is known to have a significant effect on fatigue and imprint. The origin of strains at phase interfaces that cause microcracking can be determined from the structure of the surface near the crack. Examples of our research addressing these issues are highlighted below.

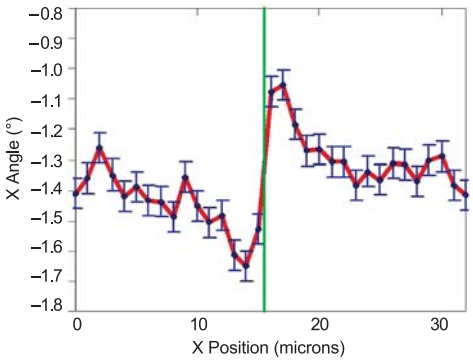

Figure 1: *Average tilt angle of lattice planes of $Al_xGa_{1-x}N$ thin films versus distance from a crack.*

A road block in the application of $Al_xGa_{1-x}N$ as light sources and detectors is the development of cracks during deposition of the films. Electron back-scatter diffraction (EBSD) was used to characterize the misorientation around individual cracks in 0.25 μm – 1.2 μm thick AlGaN films on (111) silicon substrates. EBSD showed that the orientation of the AlGaN in the vicinity of each crack changed so that lattice planes in the film tilted away from the crack causing uplift of the specimen surface, which was also seen by atomic force microscopy (AFM). The basal plane orientation change across the cracks was typically 0.6° (Figure 1) with a measurement accuracy of the order of 0.05°. The width of the strain field varied from 2 μm to 15 μm in different specimens.

The presence of impurities or an intergranular liquid phase can significantly alter properties by affecting the motion of grain boundaries and transport or conductivity between grains. We have studied the influence of boundary misorientation and chemistry on the velocity of interfaces in $SrTiO_3$ single crystals of varying orientations. Crystals were bonded to dense textured polycrystalline $SrTiO_3$ ceramics; upon heating, the interface migrates into the ceramic. This experiment allows the isolation of key variables including crystallographic misorientation, impurity content, curvature, and boundary energy, leading to control over the nature of the grain boundaries, and the potential for improved properties.

Piezo-force microscopy (PFM) is used for characterizing individual domain orientations and the piezoelectric coefficient of ferroelectric thin films. Interpretation of results is complicated by highly localized, short-range interactions acting at the tip, as well as long-range interactions acting along the lever. The resulting distributed loads change the load applied at the tip by a factor of ≈ 3/8. Of greater importance is the impact of distributed loading on the angle along the lever. PFM measurements of piezoactuation can differ substantially from the true piezoactuation under conditions that have been modeled. Model calculations are supported by AFM measurements performed with interferometric lever detection and by PFM measurements on lead zirconate titanate thin films and triglycine sulfate crystals.

Silicon oxide-nitride-oxide multilayers are potential materials for charge storage structures in non-volatile memory devices; individual layers are 5 nm to 10 nm thick. Thorough microscopic examination of multilayers using electron energy loss spectroscopy, secondary ion mass spectrometry, and x-ray absorption spectroscopy revealed numerous details of the interface structure as a function of processing. There is a broadening of the nitrogen distribution across the nitride/oxide interfaces and reduction of the hydrogen content with increasing thermal budget in processing the top oxide. Also, radial-distribution functions are similar for differently processed silicon oxide layers.

Contributors and Collaborators

I. Levin, B. Huey, A. Scotch, D. Yoder (Ceramics Division, NIST); A. Davydov (Metallurgy Division, NIST); R. Leapman (National Institutes of Health, NIH); M. Kovler (Tower Semiconductor, Ltd.); W. Dawson, E. Sabolsky (NexTech Materials, Ltd.)

Wide Band Gap/Optoelectronic Materials

The Optoelectronics Industry Development Association roadmaps cite the need for standard reference materials (SRMs) and measurement methods to calibrate deposition processes and evaluate material properties. This project addresses those needs in the following areas: photoluminescence measurements of $Al_xGa_{1-x}As$ films for SRMs; photoreflectance measurements of band gap in InGaAsN; cathodoluminescence measurements to assess film quality in AlGaN; and Raman and photoluminescence measurements to evaluate stress and composition in $Al_xGa_{1-x}As$.

Albert Paul, Lawrence Robins, and Grady White

The NIST program to produce $Al_xGa_{1-x}As$ standard reference materials (SRMs) for the optoelectronics industry is nearing completion. Photoluminescence (PL) determined compositions of $Al_xGa_{1-x}As/Ge$ films and AlGaAs lift-off films have been compared with results of inductively-coupled-plasma optical-emission spectroscopy (ICP–OES) measurements made in the Analytical Chemistry Division at NIST. Although Ge substrates eliminated biasing the ICP–OES results with Ga or As from GaAs substrates, there was concern that the Ge substrates would alter the $Al_xGa_{1-x}As$ band gaps. However, PL measurements confirmed that band gap energies for AlGaAs/Ge agreed with AlGaAs/GaAs. $Al_{.20}Ga_{.80}As$ SRMs are to be released in September 2003.

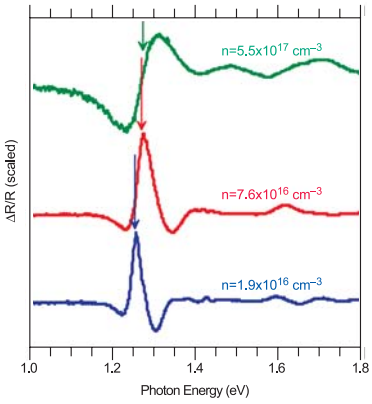

Figure 1: *PR of InGaAs films.*

Photoreflectance (PR) is a useful probe of the electronic structure of InGaAsN films, a new class of infrared optoelectronic materials. Figure 1 shows PR spectra of films with 8 % In, 0.4 % N, and varying silicon dopant and free carrier ("n") concentrations. The lines broaden and critical point energies shift upward with increasing "n". Arrows indicate the fitted band gap (lowest direct transition) energies. Higher-lying transitions (not labeled) are ascribed to splitting of both the valence and conduction bands in these alloys.

As part of a study of compositional, structural, and optical properties of AlGaN films, grown by either metalorganic chemical vapor deposition (MOCVD) or hydride vapor phase epitaxy (HVPE) on (0001) sapphire, the near-band-edge optical properties of the samples were probed by cathodoluminescence (CL) spectroscopy. Figure 2 compares low-temperature CL of films produced by different deposition processes. The near-band-edge CL lineshape is sensitive to compositional fluctuations and defect levels. The results suggest that recent HVPE grown films have improved homogeneity and crystalline quality.

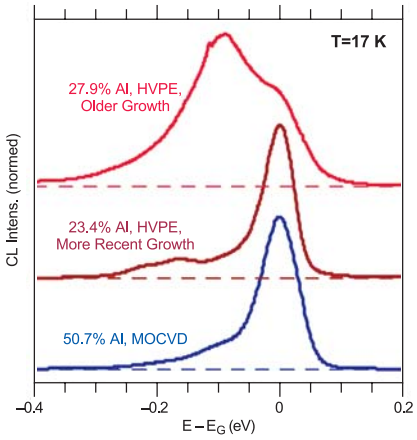

Figure 2: *CL of AlGaN films*

A paper, "Refractive Index Study of $Al_xGa_{1-x}N$ Films Grown on Sapphire Substrates," has been accepted by the *Journal of Applied Physics*.

Raman and PL spectra of $Al_xGa_{1-x}As$ have been calibrated in terms of stress and composition. Details are given in the Technical Highlights section of this report.

Contributors and Collaborators

Y.-S. Kang, M.D. Vaudin (Ceramics Division, NIST); T.A. Butler, G.C. Turk (Analytical Chemistry Division, NIST); A.V. Davydov, W.J. Boettinger, A.J. Shapiro (Metallurgy Division, NIST); K.A. Bertness, T.E. Harvey, N.A. Sanford (Optoelectronics Division, NIST); A.G. Birdwell (Semiconductor Electronics, NIST); D. Bryson, M. Fahmi, S.N. Mohammad (Howard University); S. Keller, U.K. Mishra, S.P. DenBaars (University of California, Santa Barbara); D.V. Tsvetkov, V.A. Soukoveev, A.V. Dmitriev (Technologies and Devices International, Inc.)

Materials Property Measurements

This program responds both to the Materials Science and Engineering Laboratory (MSEL) customer requests and to the Department of Commerce 2005 Strategic Goal of "providing the information and framework to enable the economy to operate efficiently and equitably." For example, manufacturers and their suppliers need to agree on how material properties should be measured. Equally important, engineering design depends on accurate property data for the materials that are used.

The MSEL Materials Property Measurement Program works toward solutions to measurement problems on scales ranging from the macro to the nano, in four of the Laboratory's Divisions (Ceramics, Materials Reliability, Metallurgy, and Polymers). The scope of its activities ranges from the development and innovative use of state-of-the-art measurement systems, to leadership in the development of standardized test procedures and traceability protocols, to the development and certification of Standard Reference Materials (SRMs). A wide range of materials is being studied, including polymers, ceramics, metals, and thin films (whose physical and mechanical properties differ widely from the handbook values for their bulk properties).

Projects are directed toward innovative new measurement techniques. These include:

- Measurement of the elastic, electric, magnetic, and thermal properties of thin films and nanostructures (Materials Reliability Division); and
- Alternative strength test methods for ceramics, including cylindrical flexure strength and diametral compression (Ceramics Division).

The MSEL Materials Property Measurement Program is also contributing to the development of test method standards through committee leadership roles in standards development organizations such as the American Society for Testing of Materials (ASTM) and the International Standards Organization (ISO). In many cases, industry also depends on measurements that can be traced to NIST Standard Reference Materials (SRMs). This program generates the following SRMs for several quite different types of measurements:

- Charpy impact machine verification (Materials Reliability Division);
- Hardness standardization of metallic materials (Metallurgy Division); and
- Hardness standardization and fracture toughness of ceramic materials (Ceramics Division).

Supporting the Materials Property Measurements Program is a modeling and simulation effort to connect microstructure with properties. The Object-Oriented Finite-Element (OOF) software developed at NIST is being used widely in diverse communities for material microstructural design and property analysis at the microstructural level.

In addition to the activities above, all four divisions provide assistance to various government agencies on homeland security and infrastructure issues. Projects include assessing the performance of structural steels as part of the NIST World Trade Center Investigation, advising the Bureau of Reclamation on metallurgical issues involving pipelines and dams, advising the Department of the Interior on the structural integrity of the U.S.S. Arizona Memorial, advising the U.S. Customs Service on materials specifications for ceramics, and advising the Architect of the Capitol on repair procedures for cracks in the outer skin of the Capitol Dome.

Contact: George Quinn

Mechanics of Materials

The reliability of brittle materials may be improved through study of their microstructure, mechanical properties, and failure mechanisms. Fractography, computational modeling tools, and transmission electron microscopy are being used to study the effects of structure, particularly the role of flaws and defects, on the strength and reliability of ceramic components.

George Quinn, Edwin Fuller, Jr., and Bernard Hockey

Ceramic materials, by virtue of their light weight, good, high-temperature performance, and broad-ranging electronic and optical properties, offer many highly desirable qualities to the designers of devices and components. However, problems can arise when high-fracture toughness or accurate lifetime prediction are required because of the inherent brittleness of most ceramics and their propensity to fail from small flaws or defects. We study the effects of microstructure on the mechanical properties of brittle materials, including microstructural features that result from such manufacturing processes as coating deposition or surface grinding or machining.

The strength of a brittle material is very often determined by the size of the largest flaw in a test specimen; large flaws concentrate stress and lower strength. In the case of ceramic parts that are brought to their final shape by an abrasive grinding process, the largest flaws can be those created at the surface by the machining process. Sometimes small changes in that process can have a dramatic effect on the strength of the part. An intensive study of damage in ground ceramic surfaces has been completed and important trends documented in NIST Special Publication 996. The telltale signs of machining cracks were identified, and schematic illustrations and simple techniques to detect these features were added as a major revision to the fractography standard ASTM C 1322. The size and severity of cracks were correlated to grinding conditions. Wheel grit size and grinding direction were reconfirmed to be dominant factors, and the effect was quantified for the first time. Grinding damage maps for silicon nitride were determined; an example is shown in Figure 1.

Another area of work concerns the structure and mechanical properties of alumina and zirconia thermal barrier coatings (TBCs). Transmission electron microscopy examination of plasma spray coatings made with submicron-sized powders revealed that the coating microstructures were very non-uniform and showed

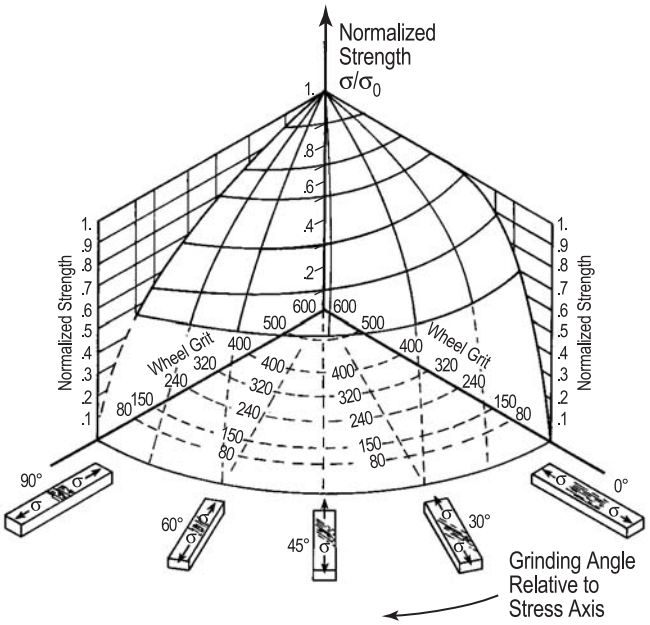

Figure 1: *Grinding damage map for silicon nitride.*

improved hardness and wear resistance relative to conventional plasma sprayed coatings. Controlled indentation flaws were also used to characterize interfacial fracture toughness in TBC systems.

Microstructure-based finite-element simulations, based on the NIST object oriented finite element (OOF) code, were used to elucidate crack–microstructure interactions. Experimental studies and corroborative OOF simulations on particulate-reinforced ceramic matrix composites showed strong crack path variations with changes in the loading/unloading rate and microstructure. OOF simulations were used to elucidate the influence of grain orientation texture on bulk physical properties (*e.g.*, coefficients of thermal expansion) and on physical behavior (*e.g.*, residual stresses and microcracking propensity). Misorientation distribution functions were shown to have a profound influence on the residual stress networks that were observed in both real and simulated microstructures.

Contributors and Collaborators

D. Saylor, L. Ives (Ceramics Division, NIST); W. Luecke (Metallurgy Division, NIST); M. Bartsch, B. Baufeld (German Aerospace Research Laboratory, Germany); S. Wu, B. Palted (University of Alabama); A. Wereszczak, M. Ferber (Oak Ridge National Lab); S. Lee (Sun Moon University, Korea)

Materials Structure Characterization

Fundamental to the field of materials science and engineering is the study of the relationships between processing, structure, properties, and performance of materials. Therefore, tools and techniques for the characterization of materials structure is a cornerstone of the field. The NIST Materials Science and Engineering Laboratory (MSEL) has a long tradition of supporting and developing measurement methods and facilities for materials structure characterization. Facilities within MSEL include optical and electron microscopy, optical and electron scattering and diffraction, a state-of-the-art x-ray diffractometer, the NIST Center for Neutron Research, and experimental stations at the National Synchrotron Light Source (NSLS) at Brookhaven Laboratory and at the Advanced Photon Source (APS) at Argonne National Laboratory. At the NSLS, NIST operates a soft x-ray station in partnership with Dow and Brookhaven National Laboratory. At the APS, NIST is a partner with the University of Illinois at Urbana/Champaign, Oak Ridge National Laboratory, and UOP in a collaboration called UNICAT. At both facilities, NIST scientists and researchers from industry, universities, and government laboratories perform state-of-the-art measurements on a wide range of advanced materials. NIST scientists have consistently advanced the limits of these facilities in order to improve spatial resolution and sensitivity needed, for example, to interrogate the microstructure of both highly anisotropic and/or gradient materials such as advanced thermal coatings and fuel cell systems. Studies currently underway at these facilities include: *in situ* measurements of nanoparticle production; structure and dispersion of carbon nanotubes; three-dimensional imaging of natural and artificial tissues; surface and subsurface damage in UV lithography optics; strain-induced ferroelectric transitions in thin films; and determination of molecular orientation and bond concentration on chemically heterogeneous surfaces.

The materials characterization program has a strong emphasis on electron microscopy. The MSEL Electron Microscopy Facility provides structure and compositional characterization of a wide range of materials. The facility consists of two transmission electron microscopes (TEMs), three scanning electron microscopes (SEMs), a specimen preparation laboratory, and an image analysis/computational laboratory. The JEM3010 TEM resolves the atomic structure and employs an energy selecting imaging filter and x-ray detector (EDS) for analytical characterization of thin foil specimens. The JSM6400 SEM employs electron backscattered diffraction/phase identification and EDS systems to characterize the texture and composition of materials. Highlights from the facility for FY2003 include: the computer domain is now active, providing streamlined user access and network file storage; a research collaboration with the NIST Semiconductor Electronics Division is underway to characterize quantum effects in confined Si devices; the size and shape of III–V quantum dots are characterized with the NIST Optoelectronics Division; and composition maps of electrodeposited nanowires with tunable magnetic properties are generated in collaboration with Johns Hopkins University.

This MSEL program also incorporates standards activities. A state-of-the-art x-ray diffractometer has been developed to study the metrology of powder diffraction in order to develop the next generation of diffraction standard reference materials. A variety of standard reference materials (SRMs) needed by the U.S. polymers industry, research laboratories, and other federal agencies have recently been developed: polyethylene of narrow mass distribution; nonlinear fluids for rheological measurements; melt flow standards; and the first reference biomaterial, an orthopedic grade ultra-high molecular weight polyethylene.

Recent program activities utilize matrix-assisted laser desorption/ionization time-of-flight mass spectrometry (MS) to address the need for improved characterization of the molecular structure of polyolefins, a dominant commercial polymer. This work has extended the upper mass limit detectable by MS to 15,000 g/mol and, by observing individual oligomeric species by mass, has revealed details of the molecular structure.

A major cross-cutting activity within this program is the multi-scale, multi-modal imaging and visualization project. The goal of this project is to combine disparate sets of 3-D imaging data that contain complementary information on overlapping length scales to produce an interactive visualization scheme for multivariate data sets. This year focused on further improvements and additions to the suite of imaging tools for tissue engineering metrology. Osteoblasts cultured in a poly (ε-caprolactone) scaffold have been imaged, demonstrating the advantages of optical coherence and confocal fluorescence microscopies over conventional laser scanning confocal microscopy. This instrument was upgraded by completely rebuilding the image acquisition software, hardware, and optical train. These improvements enabled an increase in image acquisition speed (2X) and accuracy (from 5 μm to 360 nm).

Contact: David R. Black

Diffraction Metrology and Standards

Both powder and high-resolution diffraction can provide a wealth of information with a relatively simple scan. However, the data are beset by a complex error function. It is the characterization of this function, critical to the accuracy of the technique, that is one of the prime functions of NIST diffraction Standard Reference Materials (SRMs). In order to be traceable to Systeme Internationale (SI) based units, certification measurements must be performed on equipment that features goniometers that are self-calibrating, i.e., equipped with stable, high-resolution encoders that have been calibrated using the circle closure method.

James P. Cline and Donald A. Windover

This project establishes the traceability of NIST diffraction SRMs certified with respect to lattice parameter or layer spacing. From Bragg's Law, $\lambda = 2d \sin\theta$, we see that traceability in spacing, d, requires both traceabilty in wavelength, λ, and angle, θ. The linkage of wavelength to the SI has been developed, and follows the first four levels in the traceability diagram shown in Figure 1. Here we devise a rigorous approach for the calibration of the goniometers in the Ceramics Division parallel beam diffractometer, establishing the traceabilty of angle measurement in future SRM certification.

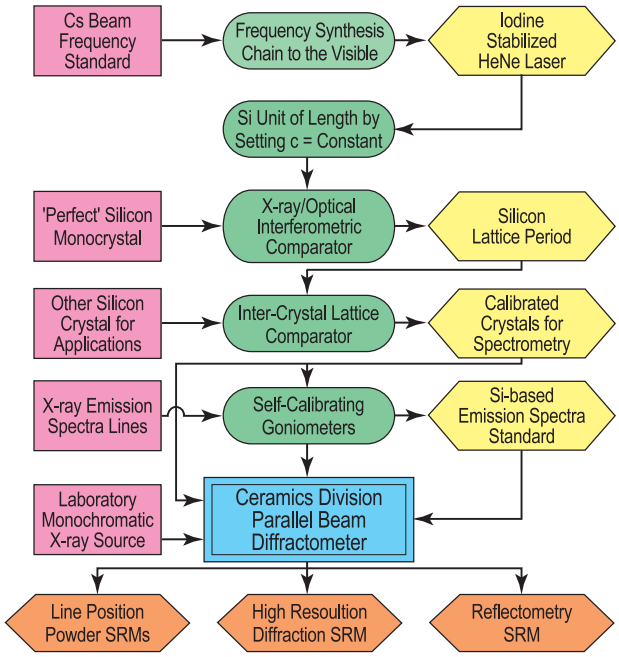

Figure 1: *Measurement chain of NIST certified diffraction SRMs.*

To be useful in a metrological context, a goniometer must have a stable, accurate and precise optical encoder. However, the encoder will exhibit an error function that must be characterized. The term "self-calibrating" refers to the ability of the goniometer to measure angles in a metrologically credible manner without relying on an external artifact and is realizable through the method of circle closure. A caveat to the method is that encoder errors must only be long range in nature, *i.e.*, caused by mounting misalignment, eccentricity, etc. In order to realize a conceptual understanding of the circle closure method, assume the goniometer of interest is equipped with a second, coaxially mounted rotation stage. This second stage rotates two optical faces, mounted parallel to the rotation axis and exhibiting a 30° dihedral angle. A scanning autocollimator is used to generate a feature associated with the angle of each face. The fitting of this feature results in a measurement precision of the angle between the faces that is much greater than that offered by the encoder itself. After each measurement, the second stage is rotated 30°, and the process repeated to yield a series of data points through 360°. Circle closure asserts that the sum of the angle measurements for one complete axis rotation must be 360°, and therefore, all errors sum to zero. Thus, the average of the measured dihedral angles provides the true angle, and deviations from this angle map the encoder correction curve.

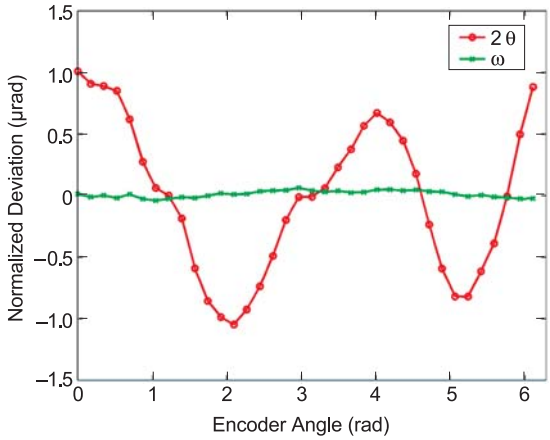

Figure 2: *Encoder error corrections from circle closure.*

We utilize a goniometer assembly with two axes of interest and a third stage for rotation of optical faces. This approach provides a matrix of encoder errors. Matrix inversion yields the calibration curves, shown in Figure 2, for the ω and 2θ goniometers.

Contributors and Collaborators

Albert Henins (Ceramics Division, NIST)

Small-Angle Scattering and Imaging

Microstructure (or nanostructure) control is the key to property and performance optimization for many materials that provide critical functions in advanced technological systems. Achieving this control requires quantitative characterization of microstructure over a contiguous size range from the nanoscale to the mesoscale. This project addresses this need by combining small-angle x-ray and neutron scattering methods with x-ray imaging capabilities to provide a microstructure-characterization-based metrology that links materials processing to performance.

Andrew Allen, Jan Ilavsky, and Gabrielle Long

New technological materials, such as those for fuel cells or thermal barrier coatings, present increasingly difficult microstructure characterization challenges. At the Advanced Photon Source (APS), as part of UNICAT (university/national laboratory/industry collaborative access team), we have made significant advances in the development of x-ray micro-tomography (XMT) and in the application of small-angle x-ray scattering (SAXS) to meet these challenges. The unique capability of the NIST ultra-SAXS (USAXS) instrument to measure absolute intensity now makes it a reference for several SAXS instruments at the APS and positions us for possible development of a SAXS standard reference material. In a continuing effort to more rapidly develop and to expand our suite of synchrotron-radiation-based x-ray characterization tools, we have developed a partnership with the X-ray Operations and Research (XOR) Division at the APS. The XMT capability at XOR serves as a proving ground for the development of nanoscale resolution XMT at UNICAT, and their capability for high-energy SAXS (HESAXS) provides increased sample penetration and spatial resolution that complement the NIST USAXS capability. Several examples of our research efforts are highlighted below.

A multi-component anisotropic-void model for USAXS analyses was used to quantify the complex microstructure of electron beam physical vapor deposited (EBPVD) thermal barrier coatings. These coatings are used in advanced gas turbine engines and are of particular interest to companies such as GE and Siemens–Westinghouse. Measurements of coatings before and after heat treatment reveal that, due to thermal expansion mismatch, a 2 % by volume population of cracks oriented normal to the substrate forms. When combined with thermal and mechanical property measurements performed by collaborators at SUNY Stony Brook, new insight has been gained into coating failure modes.

Electron-beam directed vapor deposited (EB-DVD) coatings are proposed as an alternative to conventional electron beam physical vapor-deposited coatings for high temperature thermal barrier applications. In collaboration with the University of Virginia, HESAXS has been combined with wide-angle x-ray diffraction to study EB-DVD coatings. The same sample volume was measured with both techniques at a spatial resolution of 20 μm. The measurements show that preferred crystallographic growth axes dominate near the top of the coating while void anisotropy, which plays a key role in coating durability and performance, varies throughout the thickness.

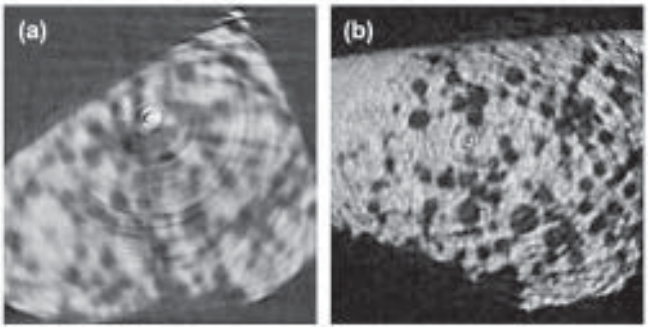

Figure 1: *XMT single-slice images through a SOFC anode layer at (a) 17 keV and (b) 27 keV x-ray energy. The 27 keV image exhibits a strong contrast between the Ni and yttria-stabilized zirconia components.*

In collaboration with the University of Utah, the structure of solid oxide fuel cell (SOFC) materials has been investigated. Measurements of pore structure and phase content have been made within each layer using USAXS, HESAXS (at 5 μm spatial resolution) and XMT. At a spatial resolution of 1.35 μm, XMT shows in 3D, for the first time, both the pore and segregated-phase size and interconnectivity actually present in the membrane layers (see Figure 1). Use of different x-ray energies allows the image contrast for different features to be optimized. This research supports current efforts to join major Department of Energy initiatives in fuel cell research.

Contributors and Collaborators

T.A. Dobbins, D.R. Black (Ceramics Division, NIST); C. Rau (Purdue University); P.R. Jemian (University of Illinois); A. Kulkarni, H. Herman (SUNY Stony Brook); C.A. Johnson (GE); D. Hass, H. Wadley (University of Virginia); A. Virkar (University of Utah); J. Almer, F. De Carlo (Argonne National Laboratory)

Synchrotron Beam Line Operation and Development

The synchrotron radiation project is focused on the operation and continued development of unique experimental facilities at the Advanced Photon Source (APS) at Argonne National Laboratory and at the National Synchrotron Light Source (NSLS) at Brookhaven National Laboratory (BNL). The emphasis is on the development and application of microstructural characterization tools and techniques that allow researchers from industry, universities and government laboratories to perform leading edge measurements on technologically advanced materials.

David R. Black

At the APS, the Ceramics Division, through UNICAT (a NIST/University of Illinois/Oak Ridge National Laboratory/UOP collaboration), supports activities in ultra-small-angle x-ray scattering (USAXS) and USAXS imaging on the insertion device line and x-ray absorption fine structure (XAFS) and diffraction topography on the bending magnet line. A hard x-ray microscope is under development. As in previous years, the USAXS instrument received the highest demand of any UNICAT instrument, with nearly 50 % of the available beam time being used for USAXS experiments. The USAXS instrument has been upgraded with an overconstrained weak-link rotational stage, which has significantly improved stability and reproducibility. The software for data reduction has been completed and the first version of software for data analysis is available on the Web. Examples of research supported by this facility include: in-situ production of nanoparticles in a flame; fuel cell microstructure; fillers for human medical implant glues; and imaging of human and artificial tissues.

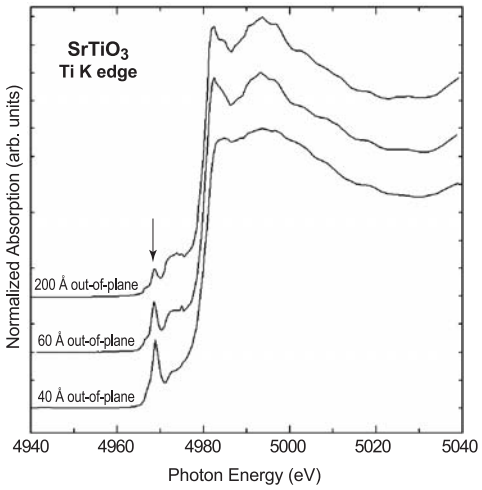

Figure 1: *XAFS data for $SrTiO_3$ thin films.*

On the bending magnet beamline, NIST researchers have used XAFS and diffraction to study $SrTiO_3$ single-crystals and thin films grown on Si (100) surfaces. Figure 1 shows the Ti-K near-edge XAFS for a series of thin films of differing thickness. The increase in the intensity of the pre-edge peak for films thinner than about 80 Å indicates hybridization of the Ti 3d and 4p states. This hybridization occurs because inversion symmetry is broken due to strain from the substrate. This "clamping effect" leads to a local ferroelectric transition in the films.

At the NSLS, the NIST/Dow beamline (U7A) is recognized as a leading materials science experimental facility on the UV ring. For the last reporting period from the NSLS, beamline U7A accounted for over 1/3 of the total number of publications reported for the UV ring.

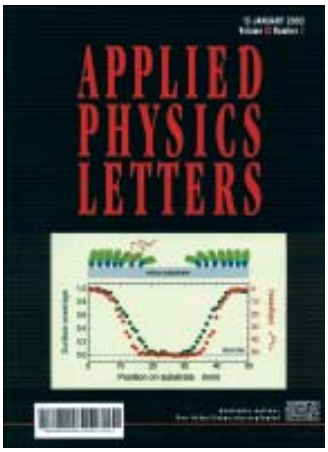

Figure 2: *Cover of Applied Physics Letters.*

Research from this facility was featured on the cover of the January 13, 2003 issue of *Applied Physics Letters*, as shown in Figure 2, "Combinatorial near-edge x-ray absorption fine structure: simultaneous determination of molecular orientation and bond concentration on chemically heterogeneous surfaces." This year, a larger and more versatile main experimental chamber was commissioned, enabling all of our unique fluorescence and electron detection capabilities to be installed simultaneously.

Contributors and Collaborators

A.J. Allen, H.E. Burdette, D.A. Fischer, G.G. Long, J.C. Woicik, D. Yoder (Ceramics Division, NIST); L.E. Levine (Metallurgy Division, NIST); S. Sambasivan (University of Delaware); J. Genzer, K. Efimenko (North Carolina State University); J. Ilavsky, C. Rau (Purdue University); P. Jemian, P. Zschack, H. Hong, J. Karapetrova (University of Illinois)

Nanocharacterization

The emphasis on nanotechnology around the world and the successful implementation of the National Nanotechnology Initiative in the U.S. are accelerating the development of science and technology at the nanoscale. Nanotechnology is expected to play a key role within the next 10 years in a wide spectrum of industry sectors including manufacturing, information technology, electronics, and healthcare. Novel devices at the micro- and nanoscale will become increasingly important in all of these industries. The ability to measure dimensions, characterize materials, and elucidate structures of new and novel materials at the nanoscale will be critical to the advancement of nanotechnology. In addition, one of the exciting prospects of nanotechnology lies in the ability of molecules or particles, under specific conditions, to self-assemble to form new materials with unusual properties. Successful development of these new materials will require the ability to monitor such processes at the nanoscale in real time. Metrology, the science of measurement, is therefore the foundation of nanotechnology. Standards and reference materials will also provide essential infrastructural support to this emerging technology.

The objective of the program in the NIST Materials Science and Engineering Laboratory (MSEL) is to develop basic measurement metrology at the nanoscale for the determination of bulk and surface material properties and for process monitoring. Measurement methods are being developed for use in conjunction with new instrumentation and calibration artifacts.

The scope of the program encompasses metals, ceramics, and polymers in various forms — particles, thin films, nanotubes, and self-assembled structures — and also includes studies of nanocomposites and liquid-state properties for microfluidics-based fabrication and measurement techniques. Physical properties such as mechanical strength, elastic moduli, friction, stiction, adhesion, and fatigue strength are measured, as well as the size of nanoparticles and the structure and dispersion behavior of nanoparticulate systems. Other properties such as electrical conductivity, thermal conductivity, magnetic properties, electronic properties, and optical properties are also examined. While the program focuses on developing measurement techniques at the nanoscale, proper data interpretation requires fundamental studies in nanomechanics, scaling laws, and imaging techniques.

There are currently ten projects under the program:

- Bridging Length Scales in Theory and Modeling;
- Electrochemical Processing of Nanoscale Materials;
- Metrology for Nanoscale Properties;
- Nanofiller Processing;
- Nanoindentation;
- Nanomechanics and Standards;
- Nanoscale Manufacturing;
- Nanotribology and Surface Properties;
- Particle Metrology and Standards; and
- Physical Properties of Thin Films and Nanostructures.

In many of these individual projects, objectives are directed toward the study of a particular class of materials or material properties, but the underlying theme of the program as a whole is to develop reliable, accurate measurement techniques for a broad range of materials and material properties at the nanoscale. As just one example, four methods for the determination of the elastic properties of thin films — atomic force acoustic microscopy, surface acoustic wave spectroscopy, Brillouin light scattering, and nanoindentation — are being compared using common sets of specimens. This study will lead to a better understanding of the complementary nature of these techniques for measuring nanostructured materials and their combined use to determine supplementary properties such as film thickness or density. Standard reference materials are being developed in collaboration with other National Measurement Institutes around the world for use in the verification of the performance of these instruments.

Contact: Stephen M. Hsu

Nanomechanics and Standards

Although much of the focus in nanotechnology is on the electronic and magnetic properties of nanoscale devices, there are many applications where device performance depends on the mechanical properties of the materials used. Stress and interfacial adhesion affect the reliability of multilayer electronic structures. Devices with micro- and nano-scale moving parts, such as cantilevers, gears and micro-mirror arrays, suffer mechanical fatigue and premature failure for reasons that are often not well understood. We develop test methods and standards for measuring mechanical properties at the nanoscale.

Douglas T. Smith

In the world of macroscopic mechanical testing, many well-characterized, standardized test methods are available to measure elastic modulus, hardness, strength, fracture toughness, adhesion, residual stress and a host of other properties critical to the successful design of reliable macroscopic structures. Often, knowledge of these same properties is just as critical to the design of micro- and nano-scale devices, but in this realm, accurate, reliable test methods for determining mechanical properties are rare. We are working on developing and evaluating techniques for mechanical property measurement, helping to draft standard test methods and developing Standard Reference Materials (SRMs) and force calibration methodology for low-force (mN down to nN) mechanical testing.

One of the most commonly used techniques for determining hardness and elastic modulus of small volumes of materials is instrumented indentation testing (IIT), often referred to as nanoindentation, in which a diamond indenter is pushed into a specimen surface and the force on, and displacement into, the surface are recorded, and those data are analyzed. The technique is capable of providing information on the elastic and plastic deformation of a specimen for indentations as shallow as 10 nm to 20 nm, and it is routinely used to measure the mechanical properties of thin films. However, until now there have been no accepted test methods that would allow IIT to be used as part of a thin-film or coating product specification. We are working with both the American Society for Testing of Materials, ASTM (E28.06.11), and the International Standards Organization, ISO (TC 164/SC 3), on draft standards for IIT; an ISO document for the technique is now at the level of Final Draft International Standard (FDIS 14577). In addition, the Ceramics and Materials Reliability Divisions at NIST are working with the Bundesanstalt für Materialforschung und–prüfung (BAM) in Germany to develop joint thin-film SRMs (CRMs, or Certified Reference Materials, in Europe) for use in IIT machine verification. This effort involves the comparison of IIT results to measurements done in the Materials Reliability Division using surface acoustic wave spectroscopy. Results on SiO_2 and TiO_2 coatings show the techniques to be in good agreement.

Other intercomparisons of thin-film mechanical test methods are underway in Technical Working Area (TWA) 22 of VAMAS (Versailles Project on Advanced Materials and Standards, **www.vamas.org**). Here, international round robin testing for hardness, elastic properties, and adhesion is being conducted to determine the reproducibility of the results between different laboratories using different commercial testing equipment.

In electronic and optoelectronic multilayer structures, delamination driven by residual stress can lead to device failure. In collaboration with the NIST Optoelectronics Division, we characterize composition and structure in III–V optoelectronic materials and are developing Raman and photoluminescence techniques for measuring residual stress in films as thin as 30 nm. Three-dimensional finite-element simulations are being used to elucidate the influence of film properties and geometry on the residual stress tensor.

In many mechanical test methods, a force is applied to a specimen, and some displacement is measured. Traceable displacement measurement by interferometry is well established. Force measurement is more problematic because the Standard International (SI) unit for force is still based on an artifact kilogram mass. The Microforce Competence Program at NIST is developing a primary realization of force, traceable to electronic and length SI units, for force calibration in the range 1 mN to 1 nN. Transfer force cells are being developed that will allow force calibration, traceable to NIST, for commercial nanomechanical test equipment such as nanoindentation machines and atomic force microscopes.

Contributors and Collaborators

B. Hockey, D. Saylor, G. White, G. Quinn, E. Fuller, S. Hsu (Ceramics Division, NIST); D. Hurley (Materials Reliability Division, NIST); B. Lawn (MSEL, NIST); K. Bertness (Optoelectronics Division, NIST); J. Pratt (Manufacturing Metrology Division, NIST); U. Beck (BAM, Germany); N. Jennett (National Physical Laboratory, U.K.); O. Takai (Nagoya University, Japan)

Nanotribology and Surface Properties

Accurate adhesion/friction measurements at the nanoscale are needed in microelectromechanical systems (MEMS) and nanoelectromechanical systems (NEMS) devices. Lubrication by molecular assemblies at nanometer dimension is required to control the surface properties of device components and ensure durability. The magnetic storage industry also needs control of friction via lubrication in the push towards 1 Terabit/in^2 areal density and a fast data transfer rate. The head-disk interface space is shrinking to 3.5 nm, with a head speed of 40 m/s. Occasional contacts between the head and disk will test the strength and robustness of the carbon overcoat and lubricant layers which are continuously being reduced in thickness.

Stephen Hsu

Significant progress has been achieved in two areas: measurements for adhesion, friction, and lubrication at the nanoscale and establishing test methods relevant to magnetic hard disk performance (with input from the National Storage Industry Consortium.)

The nanofriction measurement activity aims to develop a constitutive equation for nanofriction to include surface force components and material characteristics. We set up a novel, multiscale friction apparatus, developed jointly with Hysitron, allowing friction measurements across nm to mm scales. Figure 1 shows friction data from a diamond tip sliding on silica for different tip sizes (tip radius). The coefficient of friction values show significant dependence on tip size. Future work in nanofriction comparing results among different scales will provide an understanding of how the scale affects frictional forces.

We continue to work with our external academic partners (UC Berkeley, UC Davis, and Ohio State) under the NIST Nanotechnology Extramural Initiative. This collaboration focuses on the development of friction measurement by three approaches: MEMS devices, AFM-based methods, and a novel ultra-high vacuum method. Results thus far have revealed that meniscus forces and electrostatic forces exert a significant effect on nanofriction. We are now quantifying these effects.

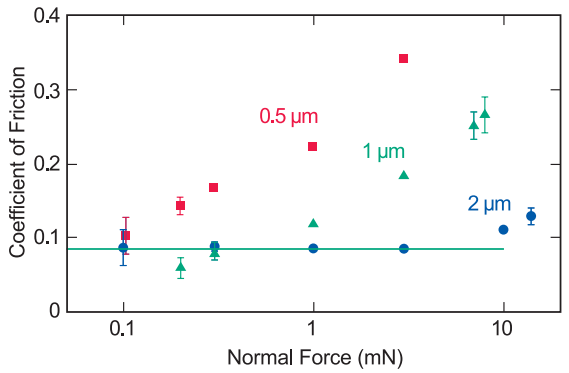

Figure 1: *Effect of tip sizes on friction.*

Significant progress has been made in establishing test methods for assessing the performance of the carbon overcoat and lubricant layers in magnetic head/disk interfaces. A high speed impact test was developed to simulate the occasional high-speed impacts that occur between the head and the disk media under the ramp-load and unload operating conditions. As the magnetic spacing continues to shrink, this type of contact could lead to data loss. In our test, a 1000 nm ridge is artificially created on a disk, and a ruby ball is used to collide with the ridge at 20 m/s. The impact force and the deformation are measured using an acoustic sensor. Recent improvements in the impact height control were achieved by installing capacitance probes to control the location and positioning of the ruby ball in the z direction. Crater imaging was also improved by using a new dual white light interferometer microscope. (See Figure 2.) Results show that the performance ranking of lubricants and overcoats agrees with field experience.

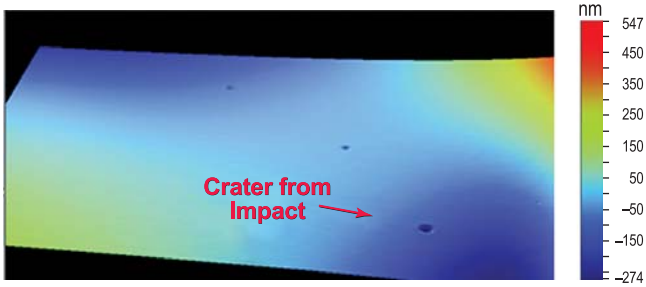

Figure 2: *Microscopic image of impact craters.*

A finite element model was developed last year to describe the stress distribution in the carbon overcoat/lubricant multilayer films. Recently, the model was improved by incorporating brittle fracture criteria for the carbon overcoat. This refinement allows the determination of the threshold stress level where data loss may occur.

Contributors and Collaborators

C. Ying, R. Gates, J. Chuang, D. Fischer (Ceramics Division, NIST); B. Bhushan (Ohio State); K. Komoupoulas (UC Berkeley); G. Liu (UC Davis); Y.T. Hsia (Seagate); J. Sengers (University of Maryland)

Particle Metrology and Standards

As technology migrates toward smaller physical dimensions, new analytical approaches are required to characterize material properties and to investigate scientifically important issues. In particle technology, these needs become critical in the nanosize regime. Industrial processes involving nanoparticle technology include advanced device manufacture and the development and production of functional materials for microelectronic, pharmaceutical, and biotechnology applications. Our goal is to improve existing metrology and develop new methods and standards for measuring the physical and interfacial properties of nanosize and nanostructured particle systems.

Vincent A. Hackley and James Kelly

Standard reference materials (SRMs) are critical for calibrating instruments used for nanoparticle characterization. Primary customers for nanoparticle SRMs are quality control laboratories in the ceramic and pharmaceutical industries. This year, we have initiated the production of a 100 nm to 500 nm particle size distribution (PSD) SRM, the first of its kind (inorganic material system with a broad size distribution), to fulfill a pressing need in the sub-micrometer size range. Interest in this TiO_2-based standard has been expressed from a wide range of industries. The SRM will be certified for PSD using electron microscopy and by X-ray disc centrifuge methods. Additionally, certification of SRM 1021 was completed. This SRM is intended for the evaluation and calibration of equipment used to measure PSDs in the 2 µm to 12 µm diameter range. The size range of this SRM follows that of the coarser beads of existing SRM 1003c.

Another activity involves ultra-small angle x-ray scattering (USAXS) of nanoparticle suspensions and partially-gelled systems. Objectives are to develop sensitive metrological techniques for characterizing metastable and unstable nanoparticle suspensions and to gain new insights into mechanisms influencing their agglomeration and stabilization. Systems of interest include SiO_2, TiO_2, and ZrO_2, studied after stabilization at pH values representing states close to and far from the isoelectric point. For example, Figure 1 shows discrete particle doublets (right-hand peak) in SiO_2 suspensions that form only at the isoelectric pH. USAXS allows such phenomena to be quantified to an unprecedented level. A flow cell for *in situ*, real-time USAXS studies of unstable suspensions is under development.

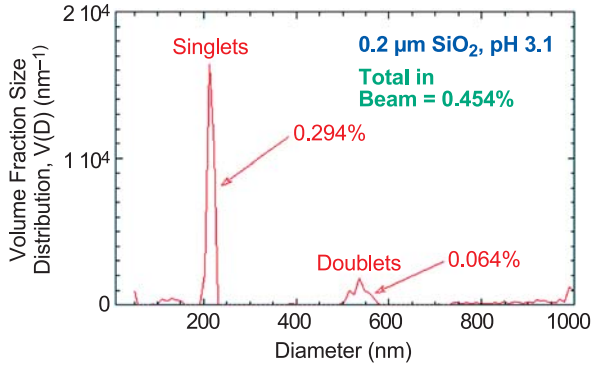

Figure 1: *Volume fraction PSD for SiO_2 at the isoelectric point.*

This year, a new activity was initiated on interfacial property measurements of nanostructured particulates. The goal is to develop the measurement methodology to obtain reliable data to establish a clear relationship between charge development and particle size, crystallinity and interparticle structure. Metal oxides exposed to an aqueous phase develop charge via protonation of surface hydroxyl sites. Surface charge and surface site reactivity play key roles in dissolution, precipitation and growth, corrosion, aggregation, and sorption processes. As particle size shrinks into the low nano-regime (< 10 nm), charge development and reactivity are predicted to exhibit size dependent behavior. Preliminary results indicate some potentially important findings.

- A systematic decrease in the isoelectric point of TiO_2 with decreasing crystallite size was observed; data will be incorporated into modeling efforts by NSF-funded researchers to account for proton-induced charge formation as a function of crystal size.
- Zeta potential measurements indicate that adducts formed between nanocrystalline MgO and molecular halogen species are more stable in an aqueous medium than had been previously predicted; this has important implications for their use as microbial biocides.
- Small-angle neutron scattering experiments suggest MgO may be capable of localized expansion around individual crystallites in response to an aqueous intrusion, without fully disrupting the assembly structure; this would represent a unique attribute not typically associated with inorganic particles.

Contributors and Collaborators

A. Allen, A. Jillavenkatesa, L. Lum (Ceramics Division, NIST); L. Sung, C. Ferraris (Materials & Construction Research Division, NIST); D. Ho (Center for Neutron Research, NIST); K. Klabunde (Kansas State University); U. Paik (Hanyang University); M. Ridley (Texas Tech University); M. Machesky (Illinois State Water Survey); P. Jemian (University of Illinois)

Ceramics Division Databases and Standards

Databases:

NIST Standard Reference Database 15: NIST/Sandia/International Centre for Diffraction Data (ICDD) Electron Diffraction Database. Chemical, physical, and crystallographic information for more than 81,500 materials, including minerals, metals, intermetallics, and general inorganic compounds; the database and associated software enable highly selective identification procedures for microscopic and macroscopic crystalline materials. (NIST Contact: V.L. Karen.) Available for purchase at **http://www.nist.gov/srd/nist15.htm**.

NIST Standard Reference Database 30: Structural Ceramics Database. Physical, mechanical, and thermal properties; more than 38,000 numeric values. (NIST contact: R.G. Munro.) Available online at **http://www.ceramics.nist.gov/srd/scd/scdquery.htm**.

NIST Standard Reference Database 31: NIST/ACerS Phase Equilibria Diagrams. Produced jointly by NIST and the American Ceramic Society; thirteen regular book volumes, five topical volumes, and a computerized database on CD ROM; more than 53,000 units have been sold; the current CD contains approximately 26,000 critically evaluated diagrams and 15,000 expert commentaries. (NIST Contact: T.A. Vanderah.) Available for purchase at **http://www.nist.gov/srd/nist31.htm**.

NIST Standard Reference Database 62: High Temperature Superconductors. Physical, mechanical, thermal, and superconducting properties; more than 30,000 numeric values. (NIST contact: R.G. Munro.) Available online at **http://www.ceramics.nist.gov/srd/hts/htsquery.htm**.

NIST Standard Reference Database 83: NIST Structural Database. Crystallographic and atomic position information for metallic crystalline substances, including alloys, intermetallics and minerals; the database is distributed in an ASCII format, convenient for reading into a variety of database management systems or processing by independent software routines. (NIST Contact: V.L. Karen.) Available for purchase at **http://www.nist.gov/srd/nist83.htm**.

NIST Standard Reference Database 84: FIZ/NIST Inorganic Crystal Structure Database, Release 2003/1 (August 2003); produced cooperatively by the Fachinformationszentrum Karlsruhe (FIZ) and NIST; a comprehensive collection of full structural crystal data of inorganic compounds; contains more than 60,000 entries. (NIST contact: V.L. Karen.) Available for purchase at **http://www.nist.gov/srd/nist84.htm**.

NIST Property Data Summaries: Focused studies with comprehensive property sets for specific materials and topical studies focused on one property for a wide range of materials. (NIST contact: R.G. Munro.) Available as follows:

Alumina, **http://www.ceramics.nist.gov/srd/summary/scdaos.htm**

Silicon Carbide, **http://www.ceramics.nist.gov/srd/summary/scdscs.htm**

Titanium Diboride, **http://www.ceramics.nist.gov/srd/summary/scdtib2.htm**

Yttrium Barium Copper Oxide, **http://www.ceramics.nist.gov/srd/summary/htsy123.htm**

Elastic Moduli Data, **http://www.ceramics.nist.gov/srd/summary/emodox00.htm**

Fracture Toughness Data, **http://www.ceramics.nist.gov/srd/summary/ftmain.htm**

Fracture Data for Oxide Glasses, **http://www.ceramics.nist.gov/srd/summary/glsmain.htm**

Standard Reference Materials:

Available for purchase at **http://ts.nist.gov/ts/htdocs/230/232/232.htm**:

Standard Reference Material 1021: Glass Beads – Particle Size Distribution, a particle size standard for size range 2 µm to 12 µm. (NIST contact: J. Kelly.)

Standard Reference Material 1003c: Glass Beads – Particle Size Distribution, a particle size standard for size range 20 µm to 50 µm. (NIST contact: J. Kelly.)

Standard Reference Material 1018b: Glass Beads – Particle Size Distribution, a particle size standard for size range 220 µm to 750 µm. (NIST contact: J. Kelly.)

Standard Reference Material 1019b: Glass Beads – Particle Size Distribution, a particle size standard for size range 750 µm to 2450 µm. (NIST contact: J. Kelly.)

Standard Reference Material 659: Particle Size Distribution for Sedigraph Calibration, a particle size standard for size range 0.2 µm to 10 µm. (NIST contact: J. Kelly.)

Standard Reference Material 8010: Sand for Sieve Analysis. (NIST contact: J. Kelly.)

Standard Reference Material 1982: Zirconia Thermal Spray Powder – Particle Size Distribution, a particle size standard for size range 10 µm to 150 µm. (NIST contact: J. Kelly.)

Standard Reference Material 1984: Thermal Spray Powder – Particle Size Distribution, Tungsten Carbide/Cobalt (Acicular), a particle size standard for size range 9 µm to 30 µm. (NIST contact: J. Kelly.)

Standard Reference Material 1985: Thermal Spray Powder – Particle Size Distribution, Tungsten Carbide/Cobalt (Spheroidal), a particle size standard for size range 18 µm to 55 µm. (NIST contact: J. Kelly.)

Standard Reference Material 2831: Vickers Hardness of Ceramics and Metals, a tungsten carbide Vickers hardness block with nominal Vickers Hardness of 15.0 GPa (1530 kgf/mm^2) for use at a testing force of 9.8 N (1.0 kgf). (NIST contact: G. Quinn.)

Measurement Standards:

ASTM C 1161, (2002): Standard Test Method for Flexural Strength of Advanced Ceramics at Ambient Temperature. (NIST contact: G. Quinn.)

ASTM C 1322, (2002): Standard Practice for Fractography and Characterization of Fracture Origins in Advanced Ceramics. (NIST contact: G. Quinn.)

ASTM F 2094, (2001): Standard Specification for Silicon Nitride Bearing Balls. (NIST contact: G. Quinn.)

ASTM C 1211, (2002): Standard Test Method for Flexural Strength of Advanced Ceramics at Ambient Temperature. (NIST contact: G. Quinn.)

ISO Standard 17565, (2001): Fine Ceramics (Advanced Ceramics, Advanced Technical Ceramics) — Test Method for Flexural Strength of Monolithic Ceramics at Elevated Temperature. (NIST contact: G. Quinn.)

ISO 18756, (2002): Fine Ceramics (Advanced Ceramics, Advanced Technical Ceramics) — Determination of Fracture Toughness of Monolithic Ceramics at Room Temperature by the Surface Crack in Flexure (SCF) Method. (NIST contact: G. Quinn.)

Ceramics Division FY03 Annual Report Publication List

Allen, A.J. "Neutron Methods Link Microstructure to Processing and Performance for Thermal Barrier Coatings." News Brief, *J. Res. Nat. Inst. Stand. Technol.*, **107**, 134 (2002).

Allen, A.J., N.F. Berk, J. Ilavsky, and G.G. Long. "Multiple Small-Angle Neutron Scattering Studies of Anisotropic Materials." *Appl. Phys. A, Mater. Sci. Process., Part 2 Suppl.*, **74**, S937–S939 (2002).

Balasubramanian, M., H.S. Lee, X. Sun, X.Q. Yang, A.R. Moodenbaugh, J. McBreen, D.A. Fischer, and Z. Fu. "Formation of Solid Electrolyte Interface on Cycled Lithium-Ion Battery Cathodes: Soft X-ray Ab-sorption Study." *Electrochemical and Solid-State Letters,* **5**, A22–A25 (2002).

Bartsch, M., B. Baufeld, and E.R. Fuller, Jr. "Elucidating Thermo-Mechanical Spallation of Thermal Barrier Coating-Systems Using Controlled Indentation Flaws." *Ceram. Eng. Sci. Proc*., **24** [3–4] (2003).

Bartsch, M., U. Schulz, J.-M. Dorvaux, O. Lavigne, E.R. Fuller, Jr., and S.A. Langer. "Simulating Thermal Response of EB-PVD Thermal Barrier Coating Microstructures." *Ceram. Eng. Sci. Proc.*, **24** [3–4] (2003).

Begley, E.F., and C.P. Sturrock. "The Background and Development of MatML, a Markup Language for Materials Property Data." *Proceedings of the 18th International CODATA Conference*, Toronto, Ontario, Canada, September 30–October 4, 2002, ICSU Committee on Data for Science and Technology, Paris, France (2002).

Belsky, A.J., M. Hellenbrandt, V.L. Karen, and P. Lucksch. "New Developments in the Inorganic Crystal Structure Database (ICSD): Accessibility in Support of Materials Research and Design." *Acta Crystallographica Section B, Structural Science*, **B58**, 364–369 (2002).

Blendell, J.E., M.R. Locatelli, J.S. Wallace and B.J. Hockey. "Modeling of Anisotropic Shrinkage During Sintering of Low Temperature Co-fired Ceramic Tapes." *IMAPS Advanced Technology Workshop on Ceramic Applications for Microwave and Photonic Packaging Report*, Providence, RI (2002).

Blendell, J.E., and J.S. Wallace, "Grain Growth in Relaxor Ferroelectrics." *AFOSR Joint Contractors Meeting Report*, Bar Harbor, ME (August 2002).

Boettinger, W.J., M.D. Vaudin, M.E. Williams, L.A. Bendersky, and W.R. Wagner. "Electron Backscattered Diffraction and Energy Dispersive X-ray Specroscopy Study of the Phase $NiSn_4$." *Journal of Electronic Materials*, **32** (6), 511–515 (2003).

Boukari, H., A.J. Allen, G.G. Long, J. Ilavsky, J.S. Wallace, C.C. Berndt, and H. Herman. "Small-Angle Neutron Scattering Study of the Role of Feedstock Particle Size on the Microstructural Behavior of Plasma-Sprayed Yttria-Stabilized Zirconia Deposits." *J. Mater. Res*., **18**, 624–634 (2003).

Burton, B.P., and A. Van de Walle. "First Principles Based Calculations of the $CaCO_3$-$MgCO_3$ Subsolidus Phase Diagrams." *Physics and Chemistry of Minerals,* **30**, 88–97 (2003).

Cedeno, C.L., and M.A. Harne. *Phase Equilibria Diagrams 2003 Cumulative Index*. Westerville, OH: The American Ceramic Society (2003).

Chawla, N., B.V. Patel, M. Koopman, K.K. Chawla, R. Saha, B.R. Patterson, E.R. Fuller, Jr., and S.A. Langer. "Microstructure-Based Simulation of Thermomechanical Behavior of Composite Materials by Object Oriented Finite (OOF) Element Analysis." *Mater. Charac*., **49,** 395–407 (2003).

Chen, C.I., and S.M. Hsu. "A Chemical Kinetic Model to Predict Lubricant Performance in a Diesel Engine. Part I: Simulation Methodology." *Tribology Letters*, **14**, No. 2, 83–90 (2003).

Ching, W.Y., Y.N. Xu, L. Ouyang, and W. Wong-Ng. "Comparative Study of the Electronic Structure of Ternary Superconductors MoRuP and ZrRuP in the Orthorhombic and Hexagonal Phases." *J. Appl Phys*., **93** (10), 8209-8211 (2003).

Choi, J.H., D.K. Kim, S.M. Wiederhorn, J.E. Blendell, B.J. Hockey, and C.A. Handwerker. "The Equilibrium Shape of Internal Cavities in Ruby and the Effect of Surface Energy Anisotropy on the Equilibrium Shape." *J. Am. Ceram. Soc.,* **85** [7], 1841–44 (2002).

Chuang, T.-J., and E.R. Fuller, Jr. "Analysis of Residual Stress State in Thermal Barrier Coatings." *Fracture Mechanics of Ceramics*, **13**, 169–178 (2003).

Chuang, T.-J., S. Jahanmir, and H.C. Tang. "Finite Element Simulation of Straight Plunge Grinding for Advanced Ceramics." *J. Europ. Ceram. Soc*., **23**, 1723–1733 (2003).

Cook, L.P., W. Wong-Ng, P. Schenck, M. Vaudin, and J. Suh. "A Model System for Interfacial Reactions in LTCC Materials." *Proceedings of IMAPS International Microelectronics and Packaging Society (IMAPS) Conference on Ceramic Interconnect Technology*, April 7–9, 2003, Denver, CO, International Microelectronics and Packaging Society, pp. 177–182 (2003).

Dieng, L.M., A.Y. Ignatov, T.A. Tyson, M. Croft, F. Dogan, C.-Y. Kim, J.C. Woicik, and J. Grow. "Observation of Changes in the Atomic and Electronic Structure of Single-Crystal $YBa_2Cu_3O_{6.6}$ Accompanying Bromination." *Phys. Rev. B,* **66**, Art. No. 14508 (2002).

Evans, C.E., A.C. Smith, D.J. Burnett, A.L. Marsh, D.A. Fischer, and J.L. Gland. "Polymer Conversion Measurement of Diacetylene-Containing Thin-Films and Monolayers using Soft X-ray Fluorescence Spectroscopy." *J. Phys. Chem. B,* **106**, 9036–9043 (2002).

Farber, L., I. Levin, A. Borisevich, I.E. Gray, R.S. Roth, and P.K. Davies. "Structural Study of Li_{1+x-y} $Nb_{1-x-3y}Ti_{x+4y}O_3$ Solid Solutions." *J. Solid State Chem.*, **166** (1), 81–90 (2002).

Ferraris, C.F., V.A. Hackley, A.I. Avilés, and C.E. Buchanan. "Analysis of the ASTM Round-Robin Test on Particle Size Distribution of Portland Cement: Phase II." NISTIR 6931, National Institute of Standards and Technology, Technology Administration, USDOC, Gaithersburg, MD (2002).

Gallagher, D.T., C. Stover, D. Charlton, L. Arnowitz, and D.R. Black. "X-ray Topography of Microgravity-Grown Rnase S Crystals." *J. Crystal Growth*, **255**/**3**–**4**, 403–413 (2003).

Genzer, J., K. Efimenko, and D.A. Fischer. "Molecular Orientation and Grafting Density in Semifluorinated Self-Assembled Monolayers of Mono-, Di- and Trichloro Silanes on Silica Substrates." *Langmuir*, **18**, 9307–9311 (2002).

Genzer, J., D.A. Fischer, and K. Efimenko, "Combinatorial Near-Edge X-Ray Absorption Fine Structure: Simultaneous Determination of Molecular Orientation and Bond Concentration on Chemically Heterogeneous Surfaces." *Applied Physics Letters,* **82**, 266–268 (2003).

Genzer, J., E.J. Kramer, and D.A. Fischer. "Accounting for Auger Yield Energy Loss for Improved Molecular Orientation Using Soft X-Ray Absorption." *J. Applied Physics*, **92**, 7070–7079 (2002).

Goyal, A., W. Wong-Ng, M. Murakami, and J. Driscoll, eds. "High Temperature Superconductor Processing." Electronics Division Focus Session at the ACerS Annual Meeting, St. Louis, MO, April 29–May 1, 2002. *Ceramics Transaction*, Vol. 140. Columbus, OH: The American Ceramic Society (2003).

Hackley, V.A., M. Naito, and R. Wäsche. "Measuring the Isoelectric Point of Ceramic Powder Suspensions: A Pre-Standardization Study." Ed. M. Matsui, S. Jahanmir, H. Mostagaci, M. Naito, K. Uematsu, R. Waesche, and R. Morrell. *Improved Ceramics Through New Measurements, Processing, and Standards, Ceramic Transactions*, **133**, 15–24, Maui, Hawaii, Nov. 4–8, 2001. Westerville, OH: The American Ceramic Society (2002).

Haugan, T.J., W. Wong-Ng, L.P. Cook, M.D. Vaudin, L. Swartzendruber, and P. Barnes. "Partial Melt Processing of Solid–Solution $Bi_2SrCaCu_2O_{8+x}$ Thick Film Conductors with Nanophase Al_2O_3 Additions." *J. Mater Res. Soc.*, **18** [5], 1054–1066 (2003).

Haugan, T.J., M.E. Fowler, J.C. Tolliver, P.N. Barnes, W. Wong-Ng, and L.P. Cook. "Flux Pinning and Properties of Solid-Solution $(Y,Nd)_{1+x}Ba_{2-x}Cu_3O_{7-z}$ Superconductors." Electronics Division Focus Session at the ACerS Annual Meeting, St. Louis, MO, April 29–May 1, 2002. Ed. A. Goyal, W. Wong-Ng, M. Murakami, and J. Driscoll. *High Temperature Superconductor Processing, Ceramics Transaction*, **140**, 299–308. Columbus, OH: The American Ceramic Society (2003).

Hockey, B.J., S.M. Wiederhorn, J.E. Blendell, J.-S. Lee, and M.-K. Kang. "Structure of Sapphire Bicrystal Boundaries Produced by Liquid-Phase Sintering." *J. Am. Ceram. Soc.,* **86** [4], 612–22 (2003).

Hsu, S.M. "Molecular Basis of Lubrication." *Proceedings of the Second Asian International Conference on Tribology,* Jeju, Korea, Oct. 21–23, 2002, KSTLE, Seoul, Korea, pp. 49–50 (2002).

Hsu, S.M., J. Zhang, and Z.F. Yin. "The Nature and Origin of Tribochemistry." *Tribology Letters*, **13**, 2, 131–139 (2002).

Hsu, S.M., R.G. Munro, and M.C. Shen. "Wear in Boundary Lubrication." *J. Engineering Tribology*, **216**, 427–441 (2002).

Hsu, S.M. "Nanotribology: the Link to Macrotribology." Ed. G.W. Stachowiak. *Proceedings of the 6th International Tribology Conference, Austrib'02: Frontiers in Tribology*, Perth, Australia, Dec. 2–5, 2002, pp. 9–16 (2002).

Hsu, S.M., and Z.C. Ying, eds. *Nanotribology: Critical Assessment and Research Directions.* New York: Kluwer Academic Press (2002).

Hsu, S.M. "Nano-Lubrication: Principle and Design." Ed. S.M. Hsu and Z.C. Ying. *Nanotribology: Critical Assessment and Research Directions,* Chap. 23, pp. 327–346. New York: Kluwer Academic Press (2002).

Hsu, S.M. "Molecular Basis of Lubrication." *Proceedings of the First U.S.–China Joint Conference on Tribology*, Beijing, China, Oct. 16–18, 2002, Tsinghua University, Beijing, China (2003).

Hsu, S.M., R.S. Gates, and D.E. Deckman. "Ceramics Lubrication." *Proceedings of 10th CIMTEC International Ceramics Congress* (2003).

Hsu, S.M., and C.I. Chen. "A Chemical Kinetic Model to Predict Diesel Engine Performance. Part II. Bench Test Procedures." *Tribology Letters*, **14**, No. 2, 91–97 (2003).

Hsueh, C.H., S. Lee, and T.-J. Chuang. "An Alternative Method of Solving Multilayer Bending Problems." *J. Appl. Mech*., **70**, 151–154 (2003).

Huang, Q.Z., V.L. Karen, A. Santoro, A., Kjekshus, J. Linden, T. Pietari, and P. Karen. "Substitution of Co^{3+} in $YBa_2Fe_3O_8$." *J. Solid State Chem.*, **172**, 73–80 (2003).

Ilavsky, J., A.J. Allen, G.G. Long, and P.R. Jemian. "Effective Pinhole-Collimated Ultrasmall-Angle X-ray Scattering Instrument for Measuring Anisotropic Microstructures." *Rev. of Sci. Instrum*., **73**, Part 2, 1660–1662 (2002).

Jeffrey, G.A., and V.L. Karen. "Crystallography." Ed. E.R. Cohen, D.R. Lide, and G.L. Trigg. *AIP Physics Desk Reference,* 3rd edition, Chap. 9, pp. 306–348. New York: Springer–Verlag (2002).

Kalin, M., S. Jahanmir, and B.J. Hockey. "Wear of Hydroxyapatite Sliding Against Glass-Infiltrated Alumina. *J. Mater. Res*., **18** [1], 27–36 (2003).

Karen, V.L., and A. Belsky. "FIZ/NIST Inorganic Crystal Structure Database." *NIST Standard Reference Database 84*, NIST, Gaithersburg, Maryland and FIZ, Karlsruhe, Germany. Released 2002/1 (August 2002), 2002/2 (February 2003), and 2003/1 (August 2003).

Karen, P., A. Kjekshus, Q. Huang, V.L. Karen, J.W. Lynn, N. Rosov, I. Natali Sora, and A. Santoro. "Neutron Powder Diffraction Study of Nuclear and Magnetic Structures of Oxidized and Reduced $YBa_2 Fe_3 O_{8+w}$." *J. Solid State Chem.,* **174**, 87–95 (2003).

Keller, T., W. Wagner, A.J. Allen, J. Ilavsky, N. Margadant, S. Siegmann, and G. Kostorz. "Characterisation of Thermally-Sprayed Metallic NiCrAlY Deposits by Multiple Small-Angle Scattering." *Appl. Phys. A, Mater. Sci. Process.*, *Part 2 Suppl.*, **74**, S975–S977 (2002).

Kim, C.-Y., M.J. Bedzyk, E.J. Nelson, J.C. Woicik, and L.E. Berman. "Site-Specific Valence Band Photoemission Study of alpha-Fe_2O_3." *Phys. Rev. B*., **66**, Art. No. 085115 (2002).

Klein, R., L.P. Cook, and W. Wong-Ng. "Enthalpies of Formation of the Strontium Plumbates $SrPbO_3$ and Sr_2PbO_4 from Solution Calorimetry and Knudsen Effusion Thermogravimetry." *J. Chemical Thermodynamics*, **34**, 2083–2092 (2002).

Kulkarni, A., Z. Wang, T. Nakamura, S. Sampath, A. Goland, H. Herman, A.J. Allen, J. Ilavsky, G.G. Long, J. Frahm, and R.W. Steinbrech. "Comprehensive Microstructural Characterization and Predictive Property Modeling of Plasma-Sprayed Zirconia Coatings." *Acta Mater.*, **51**, 2457–2475 (2003).

Lenhart, J.L., R.L. Jones, E.K. Lin, C.L. Soles, W.L. Wu, D.A. Fischer, S. Sambasivan, D.L. Goldfarb, and M. Angelopolous. "Probing Surface and Bulk Chemistry in Resist Films Using NEXAPS." *J. Vac. Sci. and Technol. B*, **20**, 2920–2926 (2002).

Lenhart, J.L., R.L. Jones, E.K. Lin, C.L. Soles, W.L. Wu, D.A. Fischer, S. Sambasivan, D.L. Goldfarb, and M. Angelopolous. "Probing Surface and Bulk De-protection in Resist Films Using NEXAFS." *Proc. ACS Div. Poly. Mat. Sci. and Eng.,* **87**, 417 (2002).

Leung, K., E. Cockayne, and A.F. Wright. "Effective Hamiltonian Study of $PbZr_{0.95}Ti_{0.05}O_3$." *Physical Review B,* **65**, 214111–24 (2002).

Levin, I., T.A. Vanderah, R. Coutts, and S.M. Bell. "Phase Equilibria and Dielectric Properties in Perovskite-Like $(1\text{-}x)LaCa_{0.5}Zr_{0.5}O_3$–$xATiO_3$ (A = Ca, Sr) Ceramics." *J. Mater. Res.*, **17** [7], 1729–1734 (2002).

Levin, I., T.J. Amos, J.C. Nino, T.A. Vanderah, C.A. Randall, M.E. Lanagan, and I.M. Reaney. "Crystal Structure of Compound $Bi_2Zn_{2/3}Nb_{4/3}O_3$." *J. Mater. Res*., **17** [6], 1406–1411 (2002).

Levin, I., J.Y. Chan, J.H. Scott, L. Farber, T.A. Vanderah, and J.E. Maslar. "Complex Polymorphic Behavior and Dielectric Properties of Perovskite-Related $Sr(Sr_{1/3}Nb_{2/3})O_3$." *J. Solid State Chem.*, 166 [1], 24–41 (2002).

Levin, I., T.G. Amos, J. Nino, T.A. Vanderah, I.M. Reaney, C.A. Randall, and M.T. Lanagan. "Crystal Structure of the Compound $Bi_2Zn_{2/3}Nb_{4/3}O_7$." *J. Materials Res*., **17**[6], 1406–1411 (2002).

Levin, I., T.G. Amos, J.C. Nino, T.A. Vanderah, C.A. Randall, and M.T. Lanagan. "Crystal Structure of an Unusual Cubic Pyrochlore $Bi_{1.5}Zn_{0.92}Nb_{1.5}O_{6.92}$." *J. Solid State Chem.,* **168**, 69–75 (2002).

Li, X., L. Andruzzi, E. Chiellini, G. Galli, C.K. Ober, A. Hexemer, E.J. Kramer, and D.A. Fischer. "Semifluorinated Aromatic Side-Group Macromolecules Polystyrene-Based Block Copolymers: Bulk Structure and Surface Orientation Studies." *Macromolecules*, **35**, 8078–8087 (2002).

Lin, Y.-S., R. Puthenkovilakam, J.P. Chang, C. Bouldin, I. Levin, N.V. Nguyen, Y. Sun, P. Pianetta, T. Conard, W. Vandervost, V. Venturo, and S. Selbrede. "Interfacial Properties of ZrO_2 on Silicon." *J. Appl. Phys.*, **93** [10], 5945–5952 (2003).

Liu, C.Y., S. Lee, and T.-J. Chuang. "Grain-Boundary Crack Growth in Interconnects with an Electric Current." *Materials Science and Engineering*, **B86**, 101–108 (2003).

Lofaj, F., S.M. Wiederhorn, G.G. Long, B.J. Hockey, P.R. Jemian, L. Browder, J. Andreason, and U. Taffner. "Non-Cavitational Tensile Creep in Silicon Nitride with Lu-Based Additives." *J. Eur. Ceram. Soc.*, **22** [14–15], 2479–2487 (2002).

Lofaj, F., D.T. Smith, G.V. Blessing, W.E. Luecke, and S.M.Wiederhorn. "Instrumented Indentation and Ultrasonic Velocity Techniques for the Evaluation of Creep Cavitation in Silicon Nitride." *J. Mater. Sci*., **38**, 1403–1412 (2003).

Mighell, A.D. "Conventional Cells: Monoclinic I- and C-centered Cells." *Acta Crystallographica*, **B59** [2], 300–302 (2003).

Mighell, A.D. "Lattice Matching (LM) — Prevention of Inadvertent Duplicate Publications of Crystal Structures." *J. Res. Natl. Inst. Stand. Technol.*, **107**, 425–429 (2002).

Mighell, A.D. "Conventional Cells — The Last Step Toward General Acceptance of Standard Conventional Cells for the Reporting of Crystallographic Data." *J. Res. Natl. Inst. Stand. Technol.*, **107**, 373–377 (2002).

Munro, R.G. "Titanium Diboride (TiB_2)." NIST Property Data Summaries, *Ceramics WebBook,* **http://www.ceramics.nist.gov/srd/summary/advmatdb.htm** (2002).

Munro, R.G. *Data Evaluation Theory and Practice for Materials Properties*. NIST Recommended Practice Guide, SP 960-11, Gaithersburg, Maryland (2003).

Munro, R.G., and C.P. Sturrock. "Structural Ceramics Database Update (April 2003)." *NISTIR 7022* and *Ceramics WebBook*, **http://www.ceramics.nist.gov/srd/scd/scdquery.htm**, Gaithersburg, Maryland (2003).

Nelson, E.J., J.C. Woicik, P. Pianetta, I.A. Vartanyants, and J.W. Cooper. "Quadrapole Effects in Core- and Valence-Photoelectron Emission from Crystalline Germanium Measured via a Spatially Modulated X-ray Interference Field." *Phys. Rev. B,* **65**, Art. No. 165219 (2002).

Newell, D.B., J.A. Kramar, J.R. Pratt, D.T. Smith, and E.R. Williams. "The NIST Microforce Realization and Measurement Project." *IEEE Transactions on Instrumentation and Measurement*, **53** [2], 508–511 (2003).

Paik, U., J.-G. Yeo, M.-H. Lee, V.A. Hackley, and Y.-G. Jung. "Dissolution and Reprecipitation of Barium at the Particulate $BaTiO_3$-Aqueous Solution Interface." *Mater. Res. Bull.*, **37**, 1623–1631 (2002).

Paik, U., V.A. Hackley, J. Lee, and S. Lee. "Effect of Poly(acrylic acid) and Poly(vinyl alcohol) on the Solubility of Colloidal $BaTiO_3$ in an Aqueous Medium." *J. Mater. Res.*, **18** [5], 1266–1274 (2003).

Park, D.-S., T.-W. Roh, B.J. Hockey, Y. Takigawa, B.-D. Han, H.-D. Kim, and Y. Yasutomi. "Two Cores in One Grain in the Microstructure of Silicon Nitride Prepared with Aligned Whisker Seeds." *J. Eur. Ceram. Soc*., **23**, 555–560 (2003).

Park, C.-W., D.-Y. Yoon, J.E. Blendell, and C.A. Handwerker. "Singular Grain Boundaries In Alumina and Their Roughening Transition." *J. Amer. Ceram. Soc*., **86** [4], 603–11 (2003).

Park, J.-K., D.-Y. Kim, H.-Y. Lee, J.E. Blendell, and C.A. Handwerker. "Crystallographic Orientation Dependent Dissolution Behavior of Sapphire in Anorthite Liquid Containing Cr_2O_3." *J. Amer. Ceram. Soc.*, **86** [6], 1014–1018 (2003).

Prosandeev, S., E. Cockayne, and B. Burton. "First Principles Studies of $KNbO_3$, $KTaO_3$, and $LiTaO_3$ Solid Solutions." Ed. R.E. Cohen. *Fundamental Physics of Ferroelectrics 2002.* AIP Conference Proceedings, **626**, 64–73. Woodbury, NY: American Institute of Physics (2002).

Prosandeev, S.A., E. Cockayne, B. Burton, V. Trepakov, S. Kapphan, M. Savinov, and L. Jastrabik. "Properties of $K_{1-x}Li_xTaO_3$ Solid Solutions; First-Principles Computations and Comparison with Experiments." *Japanese Journal of Applied Physics, Part 1,* **41**, 7179–7180 (2002).

Qiang, L., L. Wu, Y. Zhu, A.R. Moodenbaugh, G.D. Gu, M. Suenaga, Z.X. Ye, and D.A. Fischer. "Comparative Studies of MgB_2/Mg Nano-Composites and Press-Sintered MgB_2 Pellets." *IEEE Trans. on Applied Superconductivity,* **13**, 3051–3055 (2003).

Quinn, G.D., P.J. Patel, and I. Lloyd. "Effect of Loading Rate Upon Conventional Ceramic Microindentation Hardness." *J. Res. Natl. Inst. Stand. Technol.*, **107** [3], 299–306 (2002).

Quinn, G.D., P. Green, and K. Xu. "Cracking and the Indentation Size Effect for Knoop Hardness of Glasses." *J. Amer. Ceram. Soc*., **86** [3], 441–448 (2003).

Quinn, G.D., J.J. Swab, and M.J. Motyka. "Fracture Toughness of a Toughened Silicon Nitride by ASTM C 1421." *J. Am. Ceram. Soc*., **86** [6], 1043–1045 (2003).

Quinn, G.D. "Weibull Strength Scaling for Standardized Rectangular Flexure Specimens." *J. Am. Ceram. Soc*., **86** [3], 508–510 (2003).

Quinn, G.D. "Weibull Effective Volumes and Surfaces for Cylindrical Rods Loaded in Flexure." *J. Am. Ceram. Soc*., **86** [3], 475–478 (2003).

Quinn, G.D., L.K. Ives, and S. Jahanmir. "On the Fractographic Analysis of Machining Cracks in Ground Ceramics: A Case Study on Silicon Nitride." Special Publication SP 996, NIST, Gaithersburg, MD (May 2003).

Quinn, G.D., L.K. Ives, and S. Jahanmir. "Fractography Reveals Machining Cracks." *Bull. Amer. Ceram. Soc*., **82** [7], 11 (2003).

Quinn, G.D., and J.J. Swab. "Standard Practice for Fractography and Characterization of Fracture Origins in Advanced Ceramics." *Annual Book of Standards,* ASTM C 1322-02a, Vol. 15.01, ASTM. West Conshohocken, PA (2003).

Quinn, G.D. "Standard Test Method for Flexural Strength of Advanced Ceramics at Ambient Temperature." *Annual Book of Standards*, ASTM C 1161-02, Vol. 15.01, ASTM. West Conshohocken, PA (2003).

Robins, L.H., J.T. Armstrong, R.B. Marinenko, A.J. Paul, J.G. Pellegrino, and K.A. Bertness. "High-Accuracy Determination of the Dependence of the Photoluminescence Emission Energy on Alloy Composition in $Al_xGa_{1-x}As$ Films." *Journal of Applied Physics*, **93**, 3747–3759 (2003).

Robins, L.H., B. Steiner, N.A. Sanford, and C. Menoni. "Low-Electron-Energy Cathodoluminescence Study of Polishing and Etching Effects on the Optical Properties of Bulk Single-Crystal Gallium Nitride." Eds. E.T. Yu, C.M. Wetzel, J.S. Speck, A. Rizzi, and Y. Arakawa. Materials Research Society Symposium Proceedings, Pittsburgh, PA, *GaN and Related Alloys 2002*, **743**, 213–218 (2003).

Roth, R.S., ed. *Phase Diagrams for Electronic Ceramics I: Dielectric Ti, Nb, and Ta Oxide Systems*. Westerville, OH: The American Ceramic Society (2003).

Sahiner, M.A., S.W. Novak, J.C. Woicik, Y. Takamura, P.B. Griffin, and J.D. Plummer. "The Local Structure of Antimony in High Dose Antimony Implants in Silicon by XAFS and SIMS." MRS 2002 Spring Meeting, San Francisco, CA, April 1–5, 2002, *Mat. Res. Soc. Symp. Proc.*, **717**, Art. No. C3.6 (2002).

Schenck, P.K., and D.L. Kaiser. "Blazing a Trail." *Chemistry in Britain*, **39**, 45–47 (2003).

Siegrist, T., T.A.Vanderah, Ch. Svensson, and R.S. Roth. "Crystal Structure of $Ba_{27}Fe_{16}Ti_{33}O_{117}$." *Solid State Sciences,* **4**, 911–916 (2002).

Sturrock, C.P., and E.F. Begley. "MatML: A New Language for the Exchange of Materials Property Data over the World Wide Web." *AMPTIAC Quarterly*, **6**, No. 3, 7–9. Rome, NY: IIT Research Institute (2002).

Vanderah, D.J., R.S. Gates, V. Silin, D.N. Zeiger, J.T. Woodward, C.W. Meuse, G. Valincius, and B. Nickel. "Isostructural Self-Assembled Monolayers. 1. Octadecyl 1-Thiaoligo(ethylene oxides)." *Langmuir*, **19**, 2612–2620 (2003).

Vanderah, D.J., J. Arsenault, H. La, R.S. Gates, V. Silin, C.W. Meuse, and G. Valincius. "Structural Variations and Ordering Conditions for the Self-Assembled Monolayers of $HS(CH_2CH_2O_3\text{-}6CH_3$." *Langmuir*, **19**, 3752–3756 (2003).

Vanderah, T.A., T.R. Collins, W. Wong-Ng, I. Levin, R.S. Roth, and L. Farber. "Phase Equilibria and Crystal Chemistry in the $BaO\text{-}Al_2O_3\text{-}Nb_2O_5$ and $BaO\text{-}Nb_2O_5$ Systems." *J. Alloys Cmpds*., **346** (1–2), 116–128 (2002).

Vanderah, T.A. "Talking Ceramics." *Science,* **298**, 1182–1184 (2002).

Vanderah, T.A., R.S. Roth, T. Siegrist, W. Febo, J.M. Loezos, and W. Wong-Ng. "Subsolidus Phase Equilibria and Crystal Chemistry in the System $BaO\text{-}TiO_2\text{-}Ta_2O_5$." *Solid State Sciences,* **5**, 49–164 (2003).

Vaudin, M.D., G.R. Fox, and G.R. Kowach. "Accuracy and Reproducibility of X-ray Texture Measurements on Thin Films." *Magnetic and Electronic Films-Microstructure, Texture and Applications to Data Storage, Mater. Res. Soc. Proc.*, **721**, 17–23. Pittsburgh, PA (2002).

Vertanessian, A., A.J. Allen, and M.J. Mayo. "Agglomerate Formation During Drying." *J. Mater Res.*, **18**, 495–506 (2003).

Wallace, J.S., J.-M. Huh, J.E. Blendell, and C.A. Handwerker. "Grain Growth and Twin Formation in 0.74 PMN – 0.26 PT." *J. Amer. Ceram. Soc.*, **85** [6], 1581–1584 (2002).

Wallace, W.E., and D.A. Fischer. "Soft X-Ray Pho-tofragmentation of Propane." *J. Electron Spectroscopy and Related Phenomena,* **130**, 1–6 (2003).

Wang, Z., J.E. Blendell, G.S. White, and Q. Jiang. "Atomic Force Microscope Observations of Domains in Fine-Grained Bulk Lead Zirconate Titanate Ceramics." *Smart Materials and Structures,* **12**, 217–222 (2003).

Wang, W.L., S. Lee, and T.-J. Chuang. "Steady-state Crack Growth along a Grain Boundary in Interconnects with a High Electric Field Intensity." *Phil. Mag*. **A82**, 955–970 (2002).

Weiss, T., S. Siegesmund, and E.R. Fuller, Jr. "Thermal Stresses and Microcracking in Calcite and Dolomite Marbles via Finite Element Modelling." Eds. S. Siegesmund, A. Vollbrecht, and T. Weiss. *"Natural Stone, Weathering Phenomena, Conservation Strategies and Case Studies," Special Publication*, No. 205, pp. 81–94. London: Geological Society (2002).

Weiss, T., S. Siegesmund, and E.R. Fuller, Jr. "Thermal Degradation of Marble: Indications From Finite Element Modelling." *Building and Environment*, **38,** [9–10], 1251–1260 (2003).

White, G.S., E.R. Fuller, Jr., and S.W., Freiman. "Mechanical Reliability and Life Prediction for Brittle Materials." Ed. Myer Kutz. *Handbook of Materials Selection*, Chap. 28, pp. 809–828. New York: John Wiley & Sons, Inc. (2002).

White, G., and T. Tsurumi, eds. *Proceedings of the 13th IEEE International Symposium on Applications of Ferroelectrics*. Nara, Japan, May 28–June 1, 2002. IPiscataway, NJ: EEE Service Center (2003).

Wiederhorn, S.M., and E.R. Fuller, Jr. "Structural Behavior of Ceramics." Eds. B. Karihaloo and W.G. Knauss. *Comprehensive Structural Integrity, Volume 2: Fundamental Theories and Mechanisms of Failure*, Chap. 2.08, pp. 429–454. Oxford: Elsevier Science (2003).

Woicik, J.C., E.J. Nelson, L. Kronik, M. Jain, J.R. Chelikowsky, D. Heskett, L.E. Berman, and G.S. Herman. "Hybridization and Bond-Orbital Components in Site-Specific X-ray Photoelectron Spectra of Rutile TiO_2." *Phys. Rev. Lett.,* **89**, Art. No. 077401 (2002).

Wong-Ng, W., J. Suh, and L.P. Cook. "Subsolidus Phase Relationships of the $BaO\text{-}Y_2O_3\text{-}CuO_x$ System Under Carbonate-Free Conditions at $pO_2 = 100$ Pa and at $pO_2 = 21$ kPa." *Physica C*, **377**, 107–113 (2002).

Wong-Ng, W., W.Y. Ching, X. Yong-Nian, J.A. Kaduk, I. Shirotani, and L. Swartzendruber. "The Structure and Electronic Properties of the Orthorhombic MoRuP Superconductor Prepared at High Pressure." *Phy. Rev*., **B14**, 144523-1 to 144523-9 (2003).

Wong-Ng, W., J.A. Kaduk, and J. Dillingham. "Crystal Structures and Reference Diffraction Patterns of $BaSrR_4O_8$." *Powd. Diffr*., **17** (No. 3), 202–205 (2002).

Wong-Ng, W. "The 2001 Material Research Society (MRS) Fall Meeting." *Powd. Diffr*., **17** (1), 61–62 (2002).

Wong-Ng, W. "The 2002 Material Research Society (MRS) Fall Meeting." *Powd. Diffr*., **18** (1), 61–62 (2003).

Wong-Ng, W., L.P. Cook, and J. Suh. "Melting Equilibria of the $BaF_2\text{-}CuO_x$ System." *High Temperature Superconductor Processing*. Electronics Division Focus Session at the ACerS Annual Meeting, St. Louis, MO, April 29–May 1, 2002. Eds. A. Goyal, W. Wong-Ng, M. Murakami, and J. Driscoll. *Ceramics Transaction*, **140**, 385–397. Columbus, OH: The American Ceramic Society (2003).

Xu, H.H.K., J.B. Quinn, D.T. Smith, A.A. Giuseppetti, and F.C. Wichmiller. "Effects of Different Whiskers on the Reinforcement of Dental Resin Composites." *Dental Materials*, **19**, 359–367 (2003).

Zelezny, V., E. Cockayne, J. Petzelt, M.F. Limanov, D. Usvyat, V.V. Lemanov, and A.A. Volkov. "Temperature Dependence of Infrared-Active Phonons in $CaTiO_3$: A Combined Spectroscopic and First-Principles Study." *Physical Rev. B,* 66, Art. No. 224303 (2002).

Zhu, Y., A.R. Moodenbaugh, G. Schnieider, J.W. Davenport, T. Vogt, Q. Li, G. Gu, D.A. Fischer, and J. Tafto. "Unraveling the Symmetry of the Hole States Near the Fermi Level in the MgB_2 Superconductor." *Phys. Rev. Letters*, 88, Art. No. 247002 (2002).

Ceramics Division

Chief

Debra L. Kaiser
Phone: 301–975–6119
E-mail: debra.kaiser@nist.gov

Deputy Chief

David R. Black
Phone: 301–975–6119
E-mail: david.black@nist.gov

Group Leaders

Characterization Methods

David R. Black
Phone: 301–975–5976
E-mail: david.black@nist.gov

Data and Standards Technology

Ronald G. Munro
Phone: 301–975–6127
E-mail: ronald.munro@nist.gov

Electronic and Optoelectronic Materials

Grady S. White, *Acting*
Phone: 301–975–5752
E-mail: grady.white@nist.gov

Nanomechanical Properties

Douglas T. Smith
Phone: 301–975–6020
E-mail: douglas.smith@nist.gov

Nanotribology

Stephen M. Hsu
Phone: 301–975–6120
E-mail: stephen.hsu@nist.gov

Research Staff

Allen, Andrew
andrew.allen@nist.gov
Small-angle x-ray scattering
Small-angle neutron scattering
Ceramic microstructural analysis

Black, David
david.black@nist.gov
Defect microstructures
X-ray imaging

Blendell, John
john.blendell@nist.gov
Ceramic processing
Sintering and diffusion-controlled processes

Burdette, Harold
harold.burdette@nist.gov
X-ray optics
X-ray diffraction imaging
Instrumentation

Burton, Benjamin
benjamin.burton@nist.gov
Calculated phase diagrams
Dielectric ceramics

Chuang, Tze-Jer
tze-jer.chuang@nist.gov
Finite-element modeling
Lifetime predictions
Nanocontact mechanics

Cline, James
james.cline@nist.gov
Standard reference materials
High-temperature x-ray diffraction
Microstructural effects in x-ray diffraction
Rietveld refinement of x-ray diffraction data

Cockayne, Eric
eric.cockayne@nist.gov
First-principles methods
Phase equilibria and properties of dielectrics

Cook, Lawrence
lawrence.cook@nist.gov
High-temperature chemistry
Phase equilibria

Dobbins, Tabbetha
tabbetha.dobbins@nist.gov
Small-angle x-ray scattering
Small-angle neutron scattering
Ceramic microstructural analysis

Fischer, Daniel
daniel.fischer@nist.gov
Soft x-ray absorption fine structure
X-ray scattering
Surface science

Fuller, Edwin
edwin.fuller@nist.gov
Microstructural modeling and simulation
Microstructure effects on physical properties
Nanomechanical testing and properties
Toughening mechanisms

Gates, Richard
richard.gates@nist.gov
Tribo-chemistry of ceramics
Chemical analysis of ceramics
Nanometer film thickness measurements

Hackley, Vincent
vince.hackley@nist.gov
Particle characterization
Particle dispersion and interface chemistry
Visco-elastic properties of suspensions

Harris, Joyce
joyce.harris@nist.gov
Data acquisition
Digitization and data entry

Hockey, Bernard
bernard.hockey@nist.gov
Transmission electron microscopy
Nanoindentation
Microstructural and defect characterization
Structure and composition of interfaces

Hsu, Stephen
stephen.hsu@nist.gov
Nanotribology
Nanolubrication
Magnetic hard disk interface
MEMs stiction

Huey, Bryan
bryan.huey@nist.gov
Atomic force microscopy
Domain stability
Ferroelectricity

Kaiser, Debra
debra.kaiser@nist.gov
Ferroelectric oxide thin films
Combinatorial material analysis

Karen, Vicky
vicky.karen@nist.gov
Crystallographic databases
Materials informatics
Lattice theory
Structural analysis

Kelly, James
james.kelly@nist.gov
Quantitative scanning electron microscopy
Image analysis
Microstructural analysis
Powder standards

Levin, Igor
igor.levin@nist.gov
Phase transitions in electronic ceramics
Crystal structure determination
Electron microscopy

Long, Gabrielle
gabrielle.long@nist.gov
Small-angle x-ray and neutron scattering
Ceramic microstructure evolution
X-ray optics

Lufaso, Michael
michael.lufaso@nist.gov
Crystal structure–physical property correlation
Modeling and prediction of crystal structures

Lum, Lin-Sien
lin-sien.lum@nist.gov
Particle characterization
Instrumentation

Munro, Ronald
ronald.munro@nist.gov
Materials properties of advanced ceramics
Data evaluation and validation
Analysis of data relations

Paul, Albert
albert.paul@nist.gov
Laser physics
Residual stress measurement

Quinn, George
george.quinn@nist.gov
Mechanical property test standards
Standard reference materials
Fractography

Robins, Lawrence
lawrence.robins@nist.gov
Defect identification and distribution
Cathodoluminescence imaging/spectroscopy
Photoluminescence spectroscopy
Raman spectroscopy

Saylor, David
david.saylor@nist.gov
Microstructural characterization
Microstructural imaging
Grain boundary analysis

Schenck, Peter
peter.schenck@nist.gov
Emission and laser spectroscopy
Thin film deposition
Computer graphics and image analysis
Combinatorial materials analysis

Scotch, Adam
adam.scotch@nist.gov
Interfaces
Microstructural evolution
Sintering and grain growth
Electronic ceramics

Smith, Douglas
douglas.smith@nist.gov
Nanomechanics
Instrumented indentation
Surfaces forces
Adhesion

Sturrock, Charles
charles.sturrock@nist.gov
Materials informatics
Data evaluation and validation
Predictive data mining

Vanderah, Terrell
terrell.vanderah@nist.gov
Solid-state chemistry
Phase equilibria of microwave dielectrics

Vaudin, Mark
mark.vaudin@nist.gov
Electron microscopy
X-ray and electron diffraction
Modeling of grain-boundary phenomena
Dielectric films

White, Grady
grady.white@nist.gov
Residual stress measurements
Mechanical reliability
Raman spectroscopy

Windover, Donald
donald.windover@nist.gov
High-resolution x-ray diffraction
X-ray reflectometry
Standard reference materials

Woicik, Joseph
joseph.woicik@nist.gov
UV photoemission
X-ray standing waves
Surface and interface science

Wong-Ng, Winnie
winnie.wong-ng@nist.gov
X-ray crystallography and reference patterns
Phase equilibria/crystal chemistry
High temperature superconductors

Yoder, Derek
derek.yoder@nist.gov
Soft x-ray absorption fine structure
X-ray scattering
Surface science

Ying, Charles
charles.ying@nist.gov
Atomic force microscopy
Nanofriction
Adhesion

Guest Scientists and Graduate Students

Armstrong, Nicholas
University of Technology, Sydney Australia

Bai, Mingwur
Tohoku University

Bartsch, Marian
Institute for Materials Research,
German Aerospace Center

Boukari, Hacene
University of Maryland

Bryson, Damian
Howard University

Cedeno, Christina
American Ceramic Society

Cha, Kum-hwan
Yousei University

Chae, Young-Hun
Kyungpook University

Coutts, Rachel
University of Maryland

Dapkunas, Stanley
Consultant

Dillingham, Jermey
University of Maryland

Evans, Howard
Smithsonian Institution

Fang, Hsu-Wei
University of Maryland

Farabaugh, Edward
American Ceramic Society

Haller, Wolfgang
Consultant

Harne, Mary
Consultant

Hastie, John
Consultant

Henins, Albert
Consultant

Ilavsky, Jan
Purdue University

Jang, Mi-Hye
Yonsei University

Jemian, Peter
University of Illinois at Urbana/Champaign

Jillavenkatesa, Ajitkumar
Alfred University

Kang, Youn-Seon
Korea Advanced Institute of Science
and Technology

Kim, Jang Yul
Hanyang University

Kim, Min-Soo
Korea Advanced Institute of Science
and Technology

Kim, Yin Yong
Seoul National University

Kulkarni, Anand
State University of New York

Li, Xiang
Rensselaer Polytechnic Institute

Liang, Yanang
Universided Oviedo, Spain

Luong, Mario
University of Maryland

McMurdie, Howard
Consultant

Mighell, Alan
Consultant

Ondik, Helen
Consultant

Ozmen, Yilmaz
Pamukkale University, Turkey

Pei, Patrick
Consultant

Peiris, Suhithi
Naval Research Laboratory

Piermarini, Gasper
University of Maryland

Prosandeev, Serguei
Rostov State University

Przedlacki, Marcin
Warshaw University of Technology

Purushotham, Kavuri
Swinbourn University

Rajagoopalan, Arun
Rensselaer Polytechnic Institute

Rau, Christoph
Purdue University

Ritter, Joseph
Consultant

Roth, Robert
Viper Group

Seo, Chang-Eui
Korea Advanced Institute of Science and Technology

Suh, Changwon
Rensselaer Polytechnic Institute

Suh, Julia
Consultant

Swanson, Nils
American Ceramic Society

Texter, John
National Science Foundation

Wang, Xiao-lei
Tohoku University

Wang, Xuemin
American Ceramic Society

Wolfenstine, Jeffrey
U.S. Army Research Laboratory

Yang, Seung Ho
Korea Advanced Institute of Science and Technology

Yeager, Glenn
Trak Ceramics, Inc.

Ying, Tony
U.S. Mint of the Treasury Department

You, Jim
American Ceramic Society

Organizational Charts

Materials Science and Engineering Laboratory

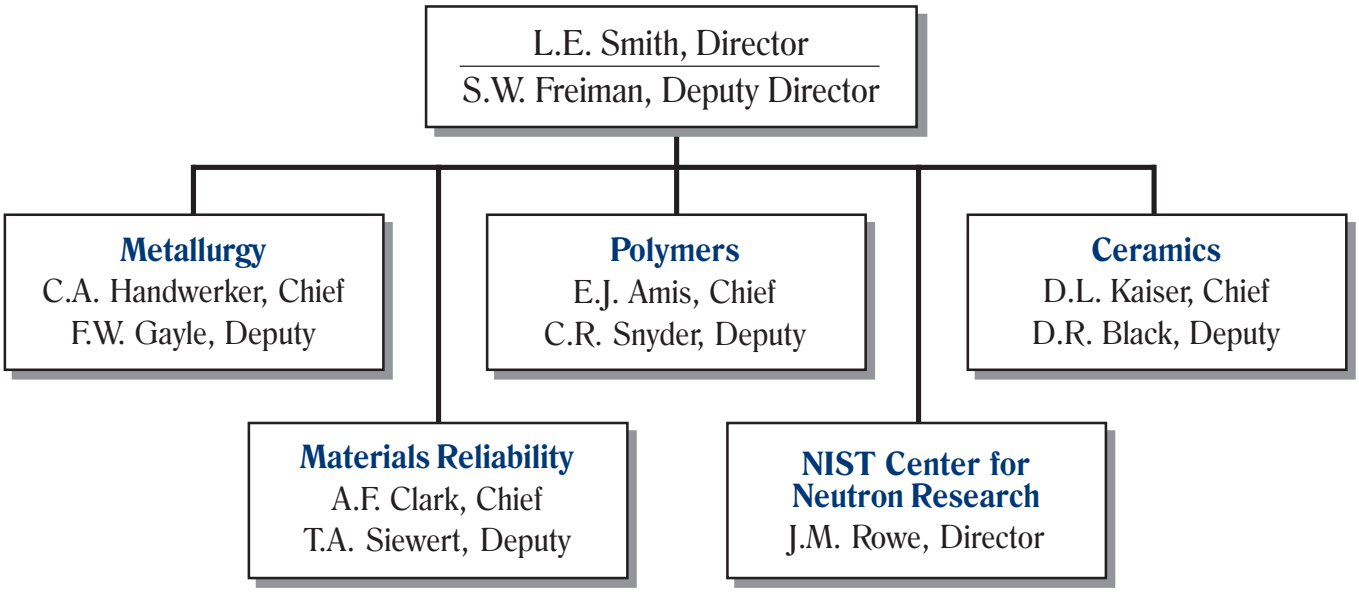

National Institute of Standards and Technology

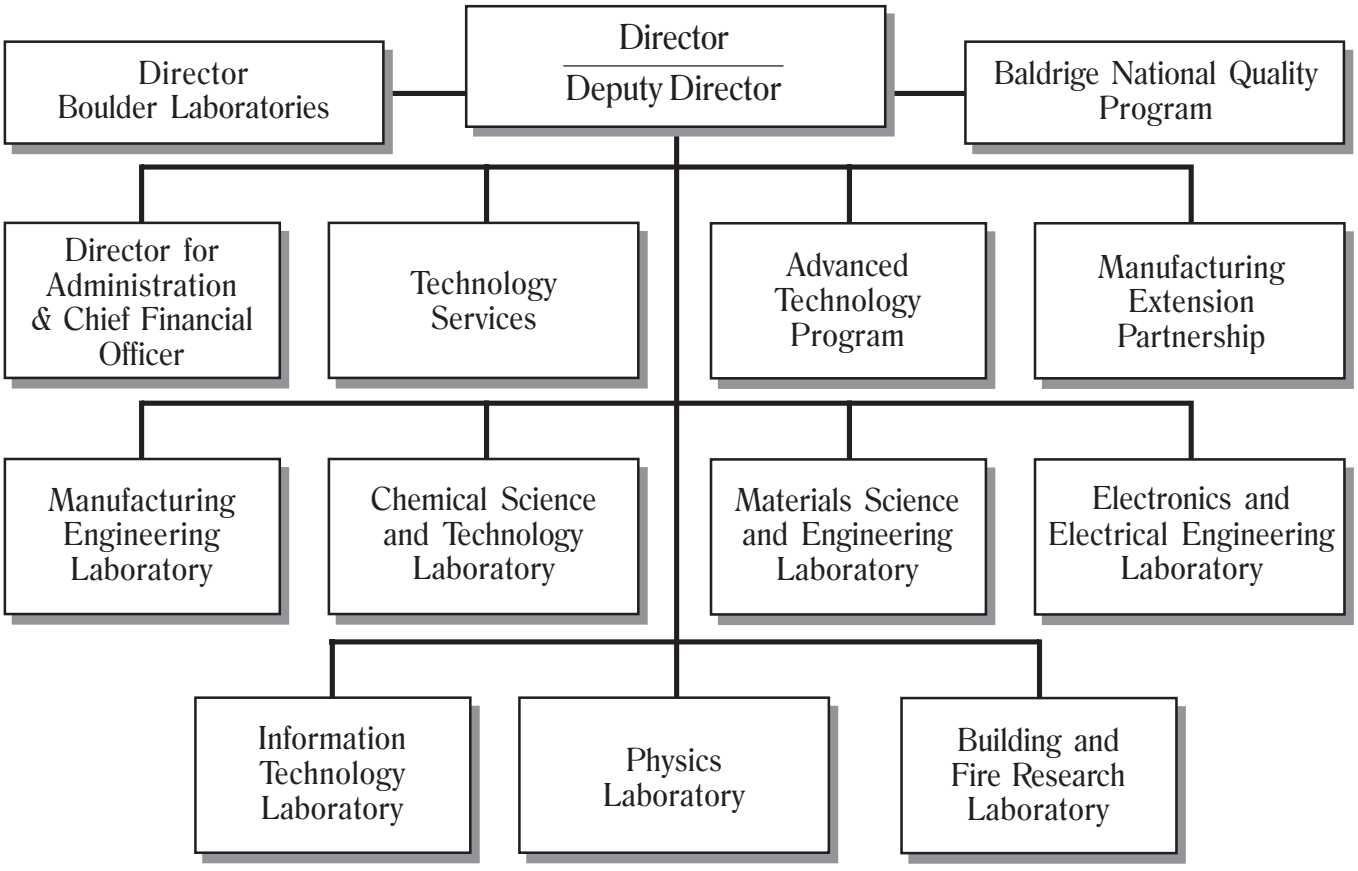

NIST